46. Suganami T, Mukoyama M, Sugawara A, Mori K, Nagae T, Kasahara M, Yahata K, Makino H, Fujinaga Y, Ogawa Y et al (2001) Overexpression of brain natriuretic peptide in mice ameliorates immune-mediated renal injury. J Am Soc Nephrol 12:2652–2663
47. Kasahara M, Mukoyama M, Sugawara A, Makino H, Suganami T, Ogawa Y, Nakagawa M, Yahata K, Goto M, Ishibashi R et al (2000) Ameliorated glomerular injury in mice overexpressing brain natriuretic peptide with renal ablation. J Am Soc Nephrol 11:1691–1701
48. Makino H, Mukoyama M, Mori K, Suganami T, Kasahara M, Yahata K, Nagae T, Yokoi H, Sawai K, Ogawa Y et al (2006) Transgenic overexpression of brain natriuretic peptide prevents the progression of diabetic nephropathy in mice. Diabetologia 49:2514–2524
49. Suda M, Ogawa Y, Tanaka K, Tamura N, Yasoda A, Takigawa T, Uehira M, Nishimoto H, Itoh H, Saito Y et al (1998) Skeletal overgrowth in transgenic mice that overexpress brain natriuretic peptide. Proc Natl Acad Sci U S A 95:2337–2342
50. Chusho H, Ogawa Y, Tamura N, Suda M, Yasoda A, Miyazawa T, Kishimoto I, Komatsu Y, Itoh H, Tanaka K et al (2000) Genetic models reveal that brain natriuretic peptide can signal through different tissue-specific receptor-mediated pathways. Endocrinology 141:3807–3813
51. Oliver PM, Fox JE, Kim R, Rockman HA, Kim HS, Reddick RL, Pandey KN, Milgram SL, Smithies O, Maeda N (1997) Hypertension, cardiac hypertrophy, and sudden death in mice lacking natriuretic peptide receptor A. Proc Natl Acad Sci U S A 94:14730–14735
52. Knowles JW, Esposito G, Mao L, Hagaman JR, Fox JE, Smithies O, Rockman HA, Maeda N (2001) Pressure-independent enhancement of cardiac hypertrophy in natriuretic peptide receptor A-deficient mice. J Clin Invest 107:975–984
53. Kishimoto I, Rossi K, Garbers DL (2001) A genetic model provides evidence that the receptor for atrial natriuretic peptide (guanylyl cyclase-A) inhibits cardiac ventricular myocyte hypertrophy. Proc Natl Acad Sci U S A 98:2703–2706
54. Holtwick R, Gotthardt M, Skryabin B, Steinmetz M, Potthast R, Zetsche B, Hammer RE, Herz J, Kuhn M (2002) Smooth muscle-selective deletion of guanylyl cyclase-A prevents the acute but not chronic effects of ANP on blood pressure. Proc Natl Acad Sci U S A 99:7142–7147
55. Holtwick R, van Eickels M, Skryabin BV, Baba HA, Bubikat A, Begrow F, Schneider MD, Garbers DL, Kuhn M (2003) Pressure-independent cardiac hypertrophy in mice with cardiomyocyte-restricted inactivation of the atrial natriuretic peptide receptor guanylyl cyclase-A. J Clin Invest 111:1399–1407
56. Sabrane K, Kruse MN, Fabritz L, Zetsche B, Mitko D, Skryabin BV, Zwiener M, Baba HA, Yanagisawa M, Kuhn M (2005) Vascular endothelium is critically involved in the hypotensive and hypovolemic actions of atrial natriuretic peptide. J Clin Invest 115:1666–1674
57. Tamura N, Ogawa Y, Yasoda A, Itoh H, Saito Y, Nakao K (1996) Two cardiac natriuretic peptide genes (atrial natriuretic peptide and brain natriuretic peptide) are organized in tandem in the mouse and human genomes. J Mol Cell Cardiol 28:1811–1815
58. Kuwahara K, Saito Y, Ogawa E, Takahashi N, Nakagawa Y, Naruse Y, Harada M, Hamanaka I, Izumi T, Miyamoto Y et al (2001) The neuron-restrictive silencer element-neuron-restrictive silencer factor system regulates basal and endothelin 1-inducible atrial natriuretic peptide gene expression in ventricular myocytes. Mol Cell Biol 21:2085–2097
59. Kuwahara K, Saito Y, Takano M, Arai Y, Yasuno S, Nakagawa Y, Takahashi N, Adachi Y, Takemura G, Horie M et al (2003) NRSF regulates the fetal cardiac gene program and maintains normal cardiac structure and function. EMBO J 22:6310–6321
60. Chusho H, Tamura N, Ogawa Y, Yasoda A, Suda M, Miyazawa T, Nakamura K, Nakao K, Kurihara T, Komatsu Y et al (2001) Dwarfism and early death in mice lacking C-type natriuretic peptide. Proc Natl Acad Sci U S A 98:4016–4021
61. Kronenberg HM (2003) Developmental regulation of the growth plate. Nature 423:332–336
62. Yasoda A, Komatsu Y, Chusho H, Miyazawa T, Ozasa A, Miura M, Kurihara T, Rogi T, Tanaka S, Suda M et al (2004) Overexpression of CNP in chondrocytes rescues achondroplasia through a MAPK-dependent pathway. Nat Med 10:80–86
63. Tamura N, Doolittle LK, Hammer RE, Shelton JM, Richardson JA, Garbers DL (2004) Critical roles of the guanylyl cyclase B receptor in endochondral ossification and development of female reproductive organs. Proc Natl Acad Sci USA 101:17300–17305
64. Langenickel TH, Buttgereit J, Pagel-Langenickel I, Lindner M, Monti J, Beuerlein K, Al-Saadi N, Plehm R, Popova E, Tank J et al (2006) Cardiac hypertrophy in transgenic rats expressing a dominant-negative mutant of the natriuretic peptide receptor B. Proc Natl Acad Sci U S A 103:4735–4740
65. Feil R, Lohmann SM, de Jonge H, Walter U, Hofmann F (2003) Cyclic GMP-dependent protein kinases and the cardiovascular system: insights from genetically modified mice. Circ Res 93:907–916
66. Pfeifer A, Aszodi A, Seidler U, Ruth P, Hofmann F, Fassler R (1996) Intestinal secretory defects and dwarfism in mice lacking cGMP-dependent protein kinase II. Science 274:2082–2086
67. Miyazawa T, Ogawa Y, Chusho H, Yasoda A, Tamura N, Komatsu Y, Pfeifer A, Hofmann F, Nakao K (2002) Cyclic GMP-dependent protein kinase II plays a critical role in C-type natriuretic peptide-mediated endochondral ossification. Endocrinology 143:3604–3610
68. Tsuji T, Kunieda T (2005) A loss-of-function mutation in natriuretic peptide receptor 2 (Npr2) gene is responsible for disproportionate dwarfism in cn/cn mouse. J Biol Chem 280:14288–14292
69. Sogawa C, Tsuji T, Shinkai Y, Katayama K, Kunieda T (2007) Short-limbed dwarfism: slw is a new allele of Npr2 causing chondrodysplasia. J Heredity 98:575–580
70. Jiao Y, Yan J, Jiao F, Yang H, Donahue LR, Li X, Roe BA, Stuart J, Gu W (2007) A single nucleotide mutation in Nppc is associated with a long bone abnormality in Ibab mice. BMC Genet 8:16
71. Tsuji T, Kondo E, Yasoda A, Inamoto M, Kiyosu C, Nakao K, Kunieda T (2008) Hypomorphic mutation in mouse Nppc gene causes retarded bone growth due to impaired endochondral ossification. Biochem Biophys Res Commun 376:186–190
72. Superti-Furga A, Bonafe L, Rimoin DL (2001) Molecular–pathogenetic classification of genetic disorders of the skeleton. Am J Med Genet 106:282–293
73. Rousseau F, Bonaventure J, Legeai-Mallet L, Pelet A, Rozet JM, Maroteaux P, Le Merrer M, Munnich A (1994) Mutations in the gene encoding fibroblast growth factor receptor-3 in achondroplasia. Nature 371:252–254
74. Cattaneo R, Villa A, Catagni M, Tentori L (1988) Limb lengthening in achondroplasia by Ilizarov's method. Int Orthop 12:173–179
75. Yasoda A, Kitamura H, Fujii T, Kondo E, Murao N, Miura M, Kanamoto N, Komatsu Y, Arai H, Nakao K (2009) Systemic administration of C-type natriuretic peptide as a novel therapeutic strategy for skeletal dysplasias. Endocrinology 150:3138–3144
76. Igaki T, Itoh H, Suga SI, Hama N, Ogawa Y, Komatsu Y, Yamashita J, Doi K, Chun TH, Nakao K (1998) Effects of intravenously administered C-type natriuretic peptide in humans:

comparison with atrial natriuretic peptide. Hypertens Res 21:7–13
77. Bartels CF, Bukulmez H, Padayatti P, Rhee DK, van Ravenswaaij-Arts C, Pauli RM, Mundlos S, Chitayat D, Shih LY, Al-Gazali LI et al (2004) Mutations in the transmembrane natriuretic peptide receptor NPR-B impair skeletal growth and cause acromesomelic dysplasia, type Maroteaux. Am J Hum Genet 75:27–34
78. Zhang Y, Proenca R, Maffei M, Barone M, Leopold L, Friedman JM (1994) Positional cloning of the mouse obese gene and its human homologue. Nature 372:425–432
79. Friedman JM, Halaas JL (1998) Leptin and the regulation of body weight in mammals. Nature 395:763–770
80. Pelleymounter MA, Cullen MJ, Baker MB, Hecht R, Winters D, Boone T, Collins F (1995) Effects of the obese gene product on body weight regulation in ob/ob mice. Science 269:540–543
81. Halaas JL, Gajiwala KS, Maffei M, Cohen SL, Chait BT, Rabinowitz D, Lallone RL, Burley SK, Friedman JM (1995) Weight-reducing effects of the plasma protein encoded by the obese gene. Science 269:543–546
82. Campfield LA, Smith FJ, Guisez Y, Devos R, Burn P (1995) Recombinant mouse OB protein: evidence for a peripheral signal linking adiposity and central neural networks. Science 269:546–549
83. Satoh N, Ogawa Y, Katsuura G, Numata Y, Tsuji T, Hayase M, Ebihara K, Masuzaki H, Hosoda K, Yoshimasa Y et al (1999) Sympathetic activation of leptin via the ventromedial hypothalamus: leptin-induced increase in catecholamine secretion. Diabetes 48:1787–1793
84. Tartaglia LA, Dembski M, Weng X, Deng N, Culpepper J, Devos R, Richards GJ, Campfield LA, Clark FT, Deeds J et al (1995) Identification and expression cloning of a leptin receptor, OB-R. Cell 83:1263–1271
85. Ogawa Y, Masuzaki H, Isse N, Okazaki T, Mori K, Shigemoto M, Satoh N, Tamura N, Hosoda K, Yoshimasa Y et al (1995) Molecular cloning of rat obese cDNA and augmented gene expression in genetically obese Zucker fatty (fa/fa) rats. J Clin Invest 96:1647–1652
86. Takaya K, Ogawa Y, Hiraoka J, Hosoda K, Yamori Y, Nakao K, Koletsky RJ (1996) Nonsense mutation of leptin receptor in the obese spontaneously hypertensive Koletsky rat. Nat Genet 14:130–131
87. Frederich RC, Hamann A, Anderson S, Lollmann B, Lowell BB, Flier JS (1995) Leptin levels reflect body lipid content in mice: evidence for diet-induced resistance to leptin action. Nat Med 1:1311–1314
88. Maffei M, Halaas J, Ravussin E, Pratley RE, Lee GH, Zhang Y, Fei H, Kim S, Lallone R, Ranganathan S et al (1995) Leptin levels in human and rodent: measurement of plasma leptin and ob RNA in obese and weight-reduced subjects. Nat Med 1:1155–1161
89. Considine RV, Sinha MK, Heiman ML, Kriauciunas A, Stephens TW, Nyce MR, Ohannesian JP, Marco CC, McKee LJ, Bauer TL et al (1996) Serum immunoreactive-leptin concentrations in normal-weight and obese humans. N Engl J Med 334:292–295
90. Isse N, Ogawa Y, Tamura N, Masuzaki H, Mori K, Okazaki T, Satoh N, Shigemoto M, Yoshimasa Y, Nishi S et al (1995) Structural organization and chromosomal assignment of the human obese gene. J Biol Chem 270:27728–27733
91. Satoh N, Ogawa Y, Katsuura G, Tsuji T, Masuzaki H, Hiraoka J, Okazaki T, Tamaki M, Hayase M, Yoshimasa Y et al (1997) Pathophysiological significance of the obese gene product, leptin, in ventromedial hypothalamus (VMH)-lesioned rats: evidence for loss of its satiety effect in VMH-lesioned rats. Endocrinology 138:947–954
92. Imagawa K, Numata Y, Katsuura G, Sakaguchi I, Morita A, Kikuoka S, Matumoto Y, Tsuji T, Tamaki M, Sasakura K et al (1998) Structure–function studies of human leptin. J Biol Chem 273:35245–35249
93. Caro JF, Kolaczynski JW, Nyce MR, Ohannesian JP, Opentanova I, Goldman WH, Lynn RB, Zhang PL, Sinha MK, Considine RV (1996) Decreased cerebrospinal-fluid/serum leptin ratio in obesity: a possible mechanism for leptin resistance. Lancet 348:159–161
94. Halaas JL, Boozer C, Blair-West J, Fidahusein N, Denton DA, Friedman JM (1997) Physiological response to long-term peripheral and central leptin infusion in lean and obese mice. Proc Natl Acad Sci U S A 94:8878–8883
95. Tanaka T, Masuzaki H, Yasue S, Ebihara K, Shiuchi T, Ishii T, Arai N, Hirata M, Yamamoto H, Hayashi T et al (2007) Central melanocortin signaling restores skeletal muscle AMP-activated protein kinase phosphorylation in mice fed a high-fat diet. Cell Metab 5:395–402
96. Montague CT, Farooqi IS, Whitehead JP, Soos MA, Rau H, Wareham NJ, Sewter CP, Digby JE, Mohammed SN, Hurst JA et al (1997) Congenital leptin deficiency is associated with severe early-onset obesity in humans. Nature 387:903–908
97. Strobel A, Issad T, Camoin L, Ozata M, Strosberg AD (1998) A leptin missense mutation associated with hypogonadism and morbid obesity. Nat Genet 18:213–215
98. Yura S, Ogawa Y, Sagawa N, Masuzaki H, Itoh H, Ebihara K, Aizawa-Abe M, Fujii S, Nakao K (2000) Accelerated puberty and late-onset hypothalamic hypogonadism in female transgenic skinny mice overexpressing leptin. J Clin Invest 105:749–755
99. Aizawa-Abe M, Ogawa Y, Masuzaki H, Ebihara K, Satoh N, Iwai H, Matsuoka N, Hayashi T, Hosoda K, Inoue G et al (2000) Pathophysiological role of leptin in obesity-related hypertension. J Clin Invest 105:1243–1252
100. Elefteriou F, Takeda S, Ebihara K, Magre J, Patano N, Kim CA, Ogawa Y, Liu X, Ware SM, Craigen WJ et al (2004) Serum leptin level is a regulator of bone mass. Proc Natl Acad Sci U S A 101:3258–3263
101. Suganami T, Mukoyama M, Mori K, Yokoi H, Koshikawa M, Sawai K, Hidaka S, Ebihara K, Tanaka T, Sugawara A et al (2005) Prevention and reversal of renal injury by leptin in a new mouse model of diabetic nephropathy. FASEB J 19:127–129
102. Masuzaki H, Ogawa Y, Hosoda K, Miyawaki T, Hanaoka I, Hiraoka J, Yasuno A, Nishimura H, Yoshimasa Y, Nishi S et al (1997) Glucocorticoid regulation of leptin synthesis and secretion in humans: elevated plasma leptin levels in Cushing's syndrome. J Clin Endocrinol Metab 82:2542–2547
103. Masuzaki H, Ogawa Y, Sagawa N, Hosoda K, Matsumoto T, Mise H, Nishimura H, Yoshimasa Y, Tanaka I, Mori T et al (1997) Nonadipose tissue production of leptin: leptin as a novel placenta-derived hormone in humans. Nat Med 3:1029–1033
104. Sagawa N, Mori T, Masuzaki H, Ogawa Y, Nakao K (1997) Leptin production by hydatidiform mole. Lancet 350:1518–1519
105. Ogawa Y, Masuzaki H, Hosoda K, Aizawa-Abe M, Suga J, Suda M, Ebihara K, Iwai H, Matsuoka N, Satoh N et al (1999) Increased glucose metabolism and insulin sensitivity in transgenic skinny mice overexpressing leptin. Diabetes 48:1822–1829
106. Masuzaki H, Ogawa Y, Isse N, Satoh N, Okazaki T, Shigemoto M, Mori K, Tamura N, Hosoda K, Yoshimasa Y et al (1995) Human obese gene expression. Adipocyte-specific expression and regional differences in the adipose tissue. Diabetes 44:855–858
107. Ioffe E, Moon B, Connolly E, Friedman JM (1998) Abnormal regulation of the leptin gene in the pathogenesis of obesity. Proc Natl Acad Sci U S A 95:11852–11857
108. Masuzaki H, Ogawa Y, Aizawa-Abe M, Hosoda K, Suga J, Ebihara K, Satoh N, Iwai H, Inoue G, Nishimura H et al (1999) Glucose metabolism and insulin sensitivity in transgenic mice

overexpressing leptin with lethal yellow agouti mutation: usefulness of leptin for the treatment of obesity-associated diabetes. Diabetes 48:1615–1622
109. Tanaka T, Hidaka S, Masuzaki H, Yasue S, Minokoshi Y, Ebihara K, Chusho H, Ogawa Y, Toyoda T, Sato K et al (2005) Skeletal muscle AMP-activated protein kinase phosphorylation parallels metabolic phenotype in leptin transgenic mice under dietary modification. Diabetes 54:2365–2374
110. Kamohara S, Burcelin R, Halaas JL, Friedman JM, Charron MJ (1997) Acute stimulation of glucose metabolism in mice by leptin treatment. Nature 389:374–377
111. Liu L, Karkanias GB, Morales JC, Hawkins M, Barzilai N, Wang J, Rossetti L (1998) Intracerebroventricular leptin regulates hepatic but not peripheral glucose fluxes. J Biol Chem 273:31160–31167
112. Cusin I, Zakrzewska KE, Boss O, Muzzin P, Giacobino JP, Ricquier D, Jeanrenaud B, Rohner-Jeanrenaud F (1998) Chronic central leptin infusion enhances insulin-stimulated glucose metabolism and favors the expression of uncoupling proteins. Diabetes 47:1014–1019
113. Goldstein BJ (1994) Syndrome of extreme insulin resistance. In: Kahn CR, Weir GC (eds) Joslin's diabetes mellitus. Lea & Febiger, Philadelphia
114. Andreelli F, Hanaire-Broutin H, Laville M, Tauber JP, Riou JP, Thivolet C (2000) Normal reproductive function in leptin-deficient patients with lipoatrophic diabetes. J Clin Endocrinol Metab 85:715–719
115. Pardini VC, Victoria IM, Rocha SM, Andrade DG, Rocha AM, Pieroni FB, Milagres G, Purisch S, Velho G (1998) Leptin levels, beta-cell function, and insulin sensitivity in families with congenital and acquired generalized lipoatrophic diabetes. J Clin Endocrinol Metab 83:503–508
116. Moitra J, Mason MM, Olive M, Krylov D, Gavrilova O, Marcus-Samuels B, Feigenbaum L, Lee E, Aoyama T, Eckhaus M et al (1998) Life without white fat: a transgenic mouse. Genes Dev 12:3168–3181
117. Shimomura I, Hammer RE, Richardson JA, Ikemoto S, Bashmakov Y, Goldstein JL, Brown MS (1998) Insulin resistance and diabetes mellitus in transgenic mice expressing nuclear SREBP-1c in adipose tissue: model for congenital generalized lipodystrophy. Genes Dev 12:3182–3194
118. Ebihara K, Ogawa Y, Masuzaki H, Shintani M, Miyanaga F, Aizawa-Abe M, Hayashi T, Hosoda K, Inoue G, Yoshimasa Y et al (2001) Transgenic overexpression of leptin rescues insulin resistance and diabetes in a mouse model of lipoatrophic diabetes. Diabetes 50:1440–1448
119. Kobayashi H, Ogawa Y, Shintani M, Ebihara K, Shimodahira M, Iwakura T, Hino M, Ishihara T, Ikekubo K, Kurahachi H et al (2002) A novel homozygous missense mutation of melanocortin-4 receptor (MC4R) in a Japanese woman with severe obesity. Diabetes 51:243–246
120. Vaisse C, Clement K, Durand E, Hercberg S, Guy-Grand B, Froguel P (2000) Melanocortin-4 receptor mutations are a frequent and heterogeneous cause of morbid obesity. J Clin Invest 106:253–262
121. Farooqi IS, Yeo GS, Keogh JM, Aminian S, Jebb SA, Butler G, Cheetham T, O'Rahilly S (2000) Dominant and recessive inheritance of morbid obesity associated with melanocortin 4 receptor deficiency. J Clin Invest 106:271–279
122. Oral EA, Simha V, Ruiz E, Andewelt A, Premkumar A, Snell P, Wagner AJ, DePaoli AM, Reitman ML, Taylor SI et al (2002) Leptin-replacement therapy for lipodystrophy. N Engl J Med 346:570–578
123. Ebihara K, Masuzaki H, Nakao K (2004) Long-term leptin-replacement therapy for lipoatrophic diabetes. N Engl J Med 351:615–616
124. Ebihara K, Kusakabe T, Hirata M, Masuzaki H, Miyanaga F, Kobayashi N, Tanaka T, Chusho H, Miyazawa T, Hayashi T et al (2007) Efficacy and safety of leptin-replacement therapy and possible mechanisms of leptin actions in patients with generalized lipodystrophy. J Clin Endocrinol Metab 92:532–541
125. Miyanaga F, Ogawa Y, Ebihara K, Hidaka S, Tanaka T, Hayashi S, Masuzaki H, Nakao K (2003) Leptin as an adjunct of insulin therapy in insulin-deficient diabetes. Diabetologia 46:1329–1337
126. Kusakabe T, Tanioka H, Ebihara K, Hirata M, Miyamoto L, Miyanaga F, Hige H, Aotani D, Fujisawa T, Masuzaki H et al (2009) Beneficial effects of leptin on glycaemic and lipid control in a mouse model of type 2 diabetes with increased adiposity induced by streptozotocin and a high-fat diet. Diabetologia 52:675–683

Am J Physiol Endocrinol Metab 298: E930–E940, 2010.
First published September 23, 2009; doi:10.1152/ajpendo.00320.2009.

Glucocorticoid reamplification within cells intensifies NF-κB and MAPK signaling and reinforces inflammation in activated preadipocytes

Takako Ishii-Yonemoto, Hiroaki Masuzaki, Shintaro Yasue, Sadanori Okada, Chisayo Kozuka, Tomohiro Tanaka, Michio Noguchi, Tsutomu Tomita, Junji Fujikura, Yuji Yamamoto, Ken Ebihara, Kiminori Hosoda, and Kazuwa Nakao

Division of Endocrinology and Metabolism, Department of Medicine and Clinical Science, Kyoto University Graduate School of Medicine, Sakyoku, Japan

Submitted 18 May 2009; accepted in final form 16 September 2009

Ishii-Yonemoto T, Masuzaki H, Yasue S, Okada S, Kozuka C, Tanaka T, Noguchi M, Tomita T, Fujikura J, Yamamoto Y, Ebihara K, Hosoda K, Nakao K. Glucocorticoid reamplification within cells intensifies NF-κB and MAPK signaling and reinforces inflammation in activated preadipocytes. *Am J Physiol Endocrinol Metab* 298: E930–E940, 2010. First published September 23, 2009; doi:10.1152/ajpendo.00320.2009.—Increased expression and activity of the intracellular glucocorticoid-reactivating enzyme 11β-hydroxysteroid dehydrogenase type 1 (11β-HSD1) contribute to dysfunction of adipose tissue. Although the pathophysiological role of 11β-HSD1 in mature adipocytes has long been investigated, its potential role in preadipocytes still remains obscure. The present study demonstrates that the expression of 11β-HSD1 in preadipocyte-rich stromal vascular fraction (SVF) cells in fat depots from *ob/ob* and diet-induced obese mice was markedly elevated compared with lean control. In 3T3-L1 preadipocytes, the level of mRNA and reductase activity of 11β-HSD1 was augmented by TNF-α, IL-1β, and LPS, with a concomitant increase in inducible nitric oxide synthase (iNOS), monocyte chemoattractant protein-1 (MCP-1), or IL-6 secretion. Pharmacological inhibition of 11β-HSD1 and RNA interference against 11β-HSD1 reduced the mRNA and protein levels of iNOS, MCP-1, and IL-6. In contrast, overexpression of 11β-HSD1 further augmented TNF-α-induced iNOS, IL-6, and MCP-1 expression. Moreover, 11β-HSD1 inhibitors attenuated TNF-α-induced phosphorylation of NF-κB p65 and p38-, JNK-, and ERK1/2-MAPK. Collectively, the present study provides novel evidence that inflammatory stimuli-induced 11β-HSD1 in activated preadipocytes intensifies NF-κB and MAPK signaling pathways and results in further induction of proinflammatory molecules. Not limited to 3T3-L1 preadipocytes, we also demonstrated that the notion was reproducible in the primary SVF cells from obese mice. These findings highlight an unexpected, proinflammatory role of reamplified glucocorticoids within preadipocytes in obese adipose tissue.

11β-hydroxysteroid dehydrogenase type 1; preadipocyte; nuclear factor-κB; mitogen-activated protein kinase; adipose inflammation

OBESE ADIPOSE TISSUE IS CHARACTERIZED by low-grade, chronic inflammation (24, 58). In humans and rodents, it has been shown that intracellular glucocorticoid reactivation is exaggerated in obese adipose tissue (38). Two isoenzymes, 11β-hydroxysteroid dehydrogenase type 1 (11β-HSD1) and type 2 (11β-HSD2), catalyze interconversion between hormonally active cortisol and inactive cortisone (2). In particular, 11β-HSD1 is abundantly expressed in adipose tissue and preferentially reactivates cortisol from cortisone (2). In contrast, 11β-HSD2 inactivates cortisol mainly in tissues involved in water and electrolyte metabolism (60). Transgenic mice overexpressing 11β-HSD1 in adipose tissue display a cluster of fuel dyshomeostasis (61). Conversely, systemic 11β-HSD1 knockouts and adipose-specific 11β-HSD2 overexpressors, which mimic adipose-specific 11β-HSD1 knockouts, are completely protected against diabetes and dyslipidemia on a high-fat diet (14, 30, 31, 42). Interestingly, 11β-HSD1 knockout mice on a high-fat diet showed preferential accumulation of subcutaneous adipose tissue, whereas wild-type mice accumulated considerable fat pads also in visceral (mesenteric) adipose tissue (39). These findings suggest that increased activity of 11β-HSD1 in adipose tissue contributes to dysfunction of adipose tissue and subsequent metabolic derangement.

Adipose tissue is composed of mature adipocytes (~50–70% of total cells), preadipocytes (~20–40%), macrophages (~1–30%), and other cell types (22). Biopsy studies of human adipose tissue demonstrated that the distribution of adipocyte diameter is bimodal, consisting of populations of very small adipocytes ("differentiating preadipocytes") and mature adipocytes (28, 35). Interestingly, the proportion of very small adipocytes was higher in obese people compared with the lean controls (28). Notably, insulin resistance was associated with an expanded population of small adipocytes and decreased expression of differentiation marker genes, suggesting that impairment of adipocyte differentiation may contribute to obesity-associated insulin resistance (35). In this context, a potential link between preadipocyte function and pathophysiology of obese adipose tissue has recently attracted research interest (53, 57).

Many of the genes overexpressed in mature adipocytes are associated with metabolic and secretory function, whereas the most representative function of the genes overexpressed in nonmature adipocytes, i.e., stromal vascular fraction (SVF) cells, is related to inflammation and immune response (9). Macrophage infiltration into obese adipose tissue contributes to local and systemic inflammation in subjects with obesity (63, 65). Furthermore, recent research (12, 48) highlights a pathophysiological role of preadipocytes in obese adipose tissue. In the proinflammatory milieu, preadipocytes act as macrophages (11, 13), share in phagocytic activities (11), and secrete an array of inflammatory substances (13).

A pharmacological dose of glucocorticoids is widely used for anti-inflammatory therapies in human clinics (49). On the other hand, recent research is highlighting the stimulatory effects of glucocorticoids on inflammatory response. Such effects are observed at lower concentrations relevant to phys-

Address for reprint requests and other correspondence: H. Masuzaki, Division of Endocrinology and Metabolism, Dept. of Medicine and Clinical Science, Kyoto University Graduate School of Medicine, 54, Shogoin Kawaharacho, Sakyoku, Kyoto, 606-8507, Japan (e-mail: hiroaki@kuhp.kyoto-u.ac.jp).

iological stress in vivo (35, 55, 66). Therefore, the potential role of 11β-HSD1 in a variety of inflammatory responses has stimulated academic interest (10, 26). Furthermore, it is known that mature adipocytes abundantly express 11β-HSD1, which is related to adipocyte dysfunction in obese adipose tissue (44, 61). On the other hand, the role of 11β-HSD1 in SVF cells remains largely unclear.

In this context, the present study was designed to explore the expression, regulation, and pathophysiological role of 11β-HSD1 in activated preadipocytes. The results demonstrate that inflammatory stimuli-induced 11β-HSD1 reinforces NF-κB and MAPK signals and results in induction of proinflammatory molecules.

MATERIALS AND METHODS

Reagents and chemicals. All reagents were of analytical grade unless otherwise indicated. TNF-α, IL-1β, LPS, and carbenoxolone (3, 52), a nonselective inhibitor for 11β-HSD1 and 11β-HSD2, were obtained from Sigma-Aldrich (St. Louis, MO). The recently developed 11β-HSD1 selective inhibitors 3-(1-adamantyl)-5,6,7,8,9,10-hexahydro[1,2,4]triazolo[4,3-α]azocine trifluoroacetate salt (WO03/065983, inhibitor A; Merck, Whitehouse Station, NJ; Ref. 23) and 2,4,6-trichloro-*N*-(5,5-dimethyl-7-oxo-4,5,6,7-tetrahydro-1,3-benzothiazol-2-yl) benzenesulfonamide (BVT-3498; Biovitrum, Stockholm, Sweden; Ref. 25) were synthesized according to the patent information.

Polyclonal antibodies against NF-κB p65, phospho-p65, p38 MAPK, phospho-p38, ERK1/2, phospho-ERK1/2, JNK, phospho-JNK, Akt, and phospho-Akt were purchased from Cell Signaling Technology (Beverly, MA). Polyclonal antibodies against SHIP1, PP2A, and MKP-1 were purchased from Santa Cruz Biotechnology (Santa Cruz, CA). An antibody against β-actin was purchased from Upstate Biotechnology (Lake Placid, NY). Horseradish peroxidase-conjugated anti-mouse, anti-rat, and anti-rabbit IgG antibodies and ECL Plus Western blotting detection kits were purchased from Amersham Biosciences (Piscataway, NJ).

Cell culture. 3T3-L1 cells (kindly provided by Dr. H. Green and Dr. M. Morikawa, Harvard Medical School, Boston, MA) were maintained in DMEM containing 10% (vol/vol) calf serum at 37°C under 10% CO_2.

Animals. Seventeen-week-old male C57BL/6 and nine-week-old *ob/ob* mice were used for the experiments. Mice were maintained on a standard diet (F-2, 3.7 kcal/g, 12% of kcal from fat, source soybean; Funahashi Farm) or a high-fat diet (Research Diets D12493, 5.2 kcal/g, 60% of kcal from fat, source soybean/lard) under a 14:10-h light-dark cycle at 23°C. The high-fat diet was administered to the diet-induced obese (DIO) mice from 3 to 17 wk of age. Animals were allowed free access to food and water. All animal experiments were undertaken in accordance with the guidelines for animal experiments of the Kyoto University Animal Research Committee.

Isolation of SVF and the mature adipocyte fraction. Subcutaneous (SQ), mesenteric (Mes), and epididymal (Epi) fat deposits were chopped using fine scissors and digested with 2 mg/ml collagenase (Type VIII; Sigma-Aldrich) in DMEM for 1 h at 37°C under continuous shaking (170 rpm). Dispersed tissue was filtered through a nylon mesh with a pore size of 250 μm and centrifuged. Digested material was separated by centrifugation at 1,800 rpm for 5 min. The sedimented SVF and cell supernatant [mature adipocyte fraction (MAF)] were both washed with DMEM. For primary culture experiments, SVF cells from epididymal fat pads were plated in sixwell plates and cultured overnight in DMEM containing 10% (vol/vol) FBS at 37°C under 10% CO_2. After being rinsed with the medium three times, the cells were incubated with or without TNF-α, carbenoxolone, or inhibitor A for 24 h.

Quantitative real-time PCR. Total RNA was extracted using Trizol reagent (Invitrogen, Carlsbad, CA), and cDNA was synthesized using an iScript cDNA synthesis kit (Bio-Rad, Hercules, CA) according to the manufacturer's instruction. The sequences of probes and primers are summarized in Suppl. Table S1 (supplemental data for this article are available at the *Am J Physiol Endocrinol Metab* website). Taqman PCR was performed using an ABI Prism 7300 sequence detection system following the manufacturer's instructions (Applied Biosystems, Foster City, CA). mRNA levels were normalized to those of 18S rRNA.

11β-HSD1 enzyme activity assay. 11β-HSD1 acts as a reductase and reactivates cortisol from cortisone in viable cells (54). In certain substrates, however, such as tissue homogenates or the microsome fraction, 11β-HSD1 acts as a dehydrogenase and inactivates cortisol to cortisone (8). 11β-HSD1 reductase activity in intact cells was measured as reported previously (8). Cells were incubated for 24 h in serum-free DMEM, with the addition of 250 nM cortisone and tritium-labeled tracer [1,2-^{3}H]$_2$-cortisone (Muromachi Yakuhin, Kyoto, Japan) for reductase activity and 250 nM cortisol with [1,2,6,7-^{3}H]$_4$-cortisol (Muromachi Yakuhin) for dehydrogenase activity. Cortisol and cortisone were extracted using ethyl acetate, evaporated, resuspended in ethanol, separated using thin-layer chromatography in 95:5 chloroform/methanol, and quantified using autoradiography.

To validate inhibitory potency of compounds against 11β-HSD1 with the use of FreeStyle 293 cells transiently transfected with human 11β-HSD1, the enzyme activity assay was carried out with 20 mM Tris · HCl at pH 7.0, 50 μM NADPH, 5 μg protein of microsomal fraction, and 300 nM [^{3}H]cortisone for 2 h. The reaction was stopped by 18β-glycyrrhetinic acid. The labeled cortisol product was captured by mouse monoclonal anti-cortisol antibody, bound to scintillation proximity assay beads coated with protein A, and quantified in a scintillation counter.

ELISA. Monocyte chemoattractant protein-1 (MCP-1) and IL-6 concentrations in the cultured media of 3T3-L1 preadipocytes were measured using ELISA according to the manufacturer's instructions (R&D Systems, Minneapolis, MN).

Western blot analysis. Two days after confluence, 3T3-L1 preadipocytes were stimulated with 10 ng/ml TNF-α in the absence or presence of 11β-HSD1 inhibitors (50 μM carbenoxolone or 10 μM inhibitor A) for 24 h.

For primary culture experiments, SVF from epididymal fat pads were plated in sixwell plates and cultured overnight in DMEM containing 10% (vol/vol) FBS at 37°C under 10% CO_2. After being rinsed with the medium three times, the cells were incubated with or without TNF-α, carbenoxolone, or inhibitor A for 24 h.

After 2-h serum starvation, cells were treated with TNF-α for 10 min to detect NF-κB and MAPK signals. Cells were washed with ice-cold PBS and harvested in lysis buffer (1% wt/vol SDS, 60 mM Tris · HCl, 1 mM Na_3VO_4, 0.1 mg/ml aprotinin, 1 mM PMSF, and 50 nM okadaic acid at pH 6.8) and boiled at 100°C for 10 min. After centrifugation, supernatants were normalized to the protein concentration via the Bradford method and then equal amounts of protein were subjected to SDS-PAGE and immunoblot analysis.

RNA interference. We tested four different small interfering RNA (siRNA) sequences. Stealth RNAi for mouse 11β-HSD1 (MSS205244, MSS205245, and MSS205246) (Invitrogen), and RNA interference (RNAi) for mouse 11β-HSD1 originally designed by an siRNA Design Support System (TaKaRa Bio, Shiga, Japan; sense: 5′-GAAAUGGCAUAUCAUCUGUTT-3′ and antisense: 3′-TTCUUUACCGUAUAGUAGACA-5′). MSS205245 and MSS205246 did not suppress the 11β-HSD1 mRNA level effectively in preliminary experiments. Therefore, we demonstrated the data of MSS205244 [si(1)] and of the originally designed siRNA [si(2)] in this study. According to the manufacturer's protocol, 3T3-L1 preadipocytes were transfected with 10 nM siRNA in antibiotic-free medium using Lipofectamine RNAiMAX (Invitrogen). We assessed the ransfection efficiency using green fluorescent protein (GFP) detection (pmaxGFP), according to the manufacturer's instructions (Amaxa, Cologne, Germany). Fluorescent microscopic observa-

tion revealed that more than two-thirds of the cells expressed GFP (data not shown).

Expression vector. A mammalian expression vector encoding Hsd11b1 (Hsd11b1/pcDNA3.1) was constructed by inserting cDNA for mouse 11β-HSD1 into pcDNA3.1 (Invitrogen). 3T3-L1 preadipocytes were detached from culture dishes using 0.25% trypsin. Cells (5×10^6) were mixed with 2 μg plasmid in the solution provided with the cell line Nucleofector Kit V (Amaxa). pcDNA3.1/11β-HSD1 or a control vector was introduced into the cells using electroporation with a Nucleofector (Amaxa) instrument according to the manufacturer's instructions.

Statistical analysis. Data are expressed as the means ± SE of triplicate experiments. Data were analyzed using one-way ANOVA, followed by Student's *t*-tests for each pair of multiple comparisons. Differences were considered significant if $P < 0.05$.

RESULTS

Expression of 11β-HSD1 was elevated in the MAF and in SVF isolated from fat depots in ob/ob mice and DIO mice. Genetic (*ob/ob*) and dietary (DIO) obese models were analyzed. Expression of iNOS, MCP-1, and IL-6, all of which are obesity-related proinflammatory mediators (19, 29, 45, 56), was elevated in the MAF and SVF from both *ob/ob* mice and DIO mice compared with lean littermates (Fig. 1, *A* and *B*). Levels of 11β-HSD1 mRNA in the MAF from obese mice were substantially elevated compared with their lean littermates (*ob/ob*: SQ, 5-fold; Mes, 62-fold) (DIO: SQ, 24-fold; Mes, 460-fold; Fig. 1, *A* and *B*). On the other hand, levels of 11β-HSD1 mRNA in SVF from *ob/ob* mice and DIO mice were also elevated compared with their lean littermates (*ob/ob*: SQ, 3-fold; Mes, 3-fold; and DIO: SQ, 8-fold, Mes, 4-fold; Fig. 1, *A* and *B*).

TNF-α, IL-1β, and LPS augmented 11β-HSD1 mRNA expression and reductase activity in 3T3-L1 preadipocytes. When 3T3-L1 preadipocytes were treated with TNF-α (10 ng/ml) for 24 h, mRNA levels of 11β-HSD1 markedly increased (~4-fold; Fig. 2*iv*). Levels of iNOS, MCP-1, and IL-6 mRNA were concomitantly increased (50-, 70-, and 200-fold, respectively; Fig. 2, *i–iii*). IL-1β (1 ng/ml) and LPS (1,000 ng/ml) substantially augmented 11β-HSD1 mRNA expression in 3T3-L1 preadipocytes (10- and 3-fold vs. control, respectively) (Fig. 2*iv*). Reductase activity of 11β-HSD1 was augmented by TNF-α, IL-1β, and LPS compared with the control (2-, 9-, and 6-fold vs. control, respectively; $P < 0.05$; Fig. 2*v*). Based on the results of 11β-HSD1 activity, TNF-α was used at 10 ng/ml in subsequent experiments. On the other hand, 11β-HSD2 mRNA and the corresponding dehydrogenase activity were undetected not only at the baseline condition but with TNF-α, IL-1β, and LPS treatments (data not shown).

Dexamethasone decreased iNOS, MCP-1, and IL-6 mRNA and protein levels in TNF-α-treated 3T3-L1 preadipocytes. The effects of glucocorticoid on proinflammatory gene expression in TNF-α-treated 3T3-L1 preadipocytes were examined over a wide range of concentrations (10^{-10}, 10^{-9}, 10^{-8}, and 10^{-7} M), representing physiological to therapeutical levels in vivo (5). Dexamethasone (10^{-7} M) decreased mRNA levels of iNOS, MCP-1, and IL-6 (iNOS: 85 ± 2%, MCP-1: 40 ± 16%, and IL-6: 97 ± 1% reduction vs. TNF-α-treated cells) and protein levels in the media (MCP-1: 48 ± 5% and IL-6: 83 ± 1% reduction) in TNF-α-treated 3T3-L1 preadipocytes (Suppl. Fig. S1).

Pharmacological inhibition of 11β-HSD1 attenuated iNOS, MCP-1, and IL-6 mRNA and protein levels in TNF-α-treated 3T3-L1 preadipocytes. The effects of pharmacological inhibition of 11β-HSD1 on proinflammatory gene expression were examined in TNFα-treated 3T3-L1 preadipocytes. In previous in vitro studies, carbenoxolone (CBX), a nonselective inhibitor of 11β-HSD1 and 11β-HSD2, was used at concentrations from 5 to 300 μM (16, 17, 26). To date, an 11β-HSD1-specific

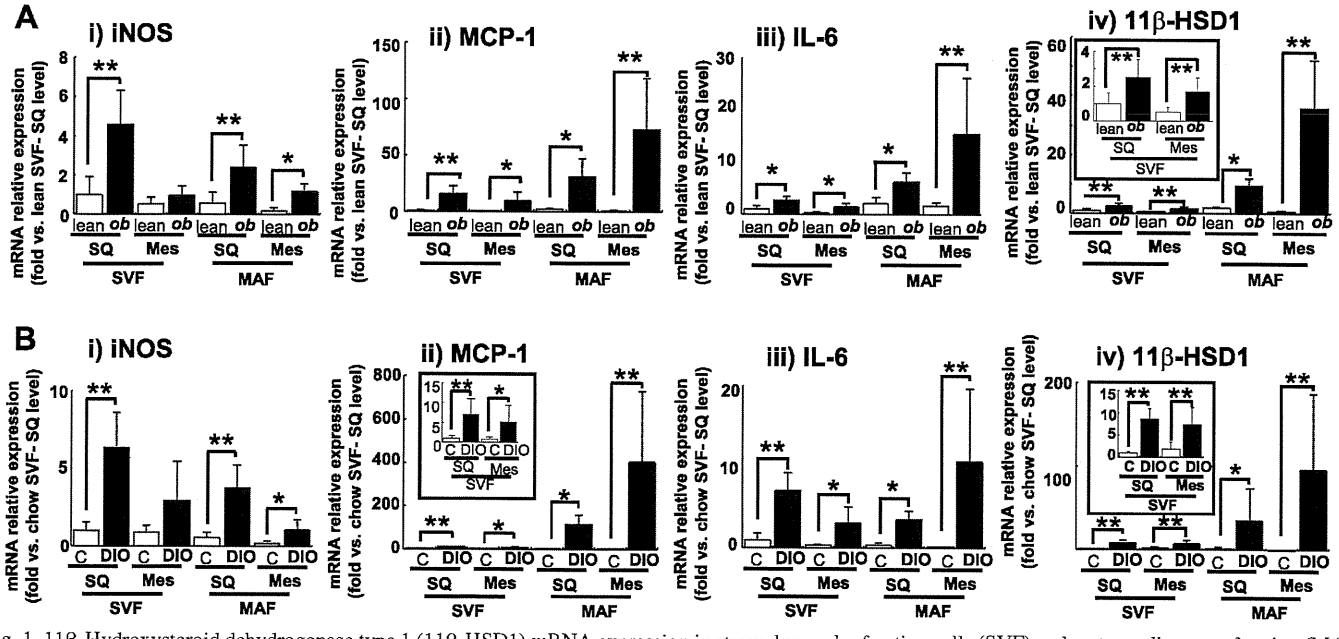

Fig. 1. 11β-Hydroxysteroid dehydrogenase type 1 (11β-HSD1) mRNA expression in stromal vascular fraction cells (SVF) and mature adipocytes fraction (MAF) isolated from obese adipose tissue of *ob/ob* mice and diet-induced obese (DIO) mice. *A*: *ob/ob* and lean littermates [control (C) 9 wk of age; $n = 6$]. *B*: DIO and littermates on a chow diet (17 wk of age; $n = 6$). Levels of inducible nitric oxide synthase (iNOS; *i*), monocyte chemoattractant protein-1 (MCP-1; *ii*), IL-6 (*iii*), and 11β-HSD1 (*iv*) mRNA in SVF and MAF in subcutaneous abdominal fat depots (SQ) and mesenteric fat depots (Mes). *$P < 0.05$, **$P < 0.01$ compared with lean littermates.

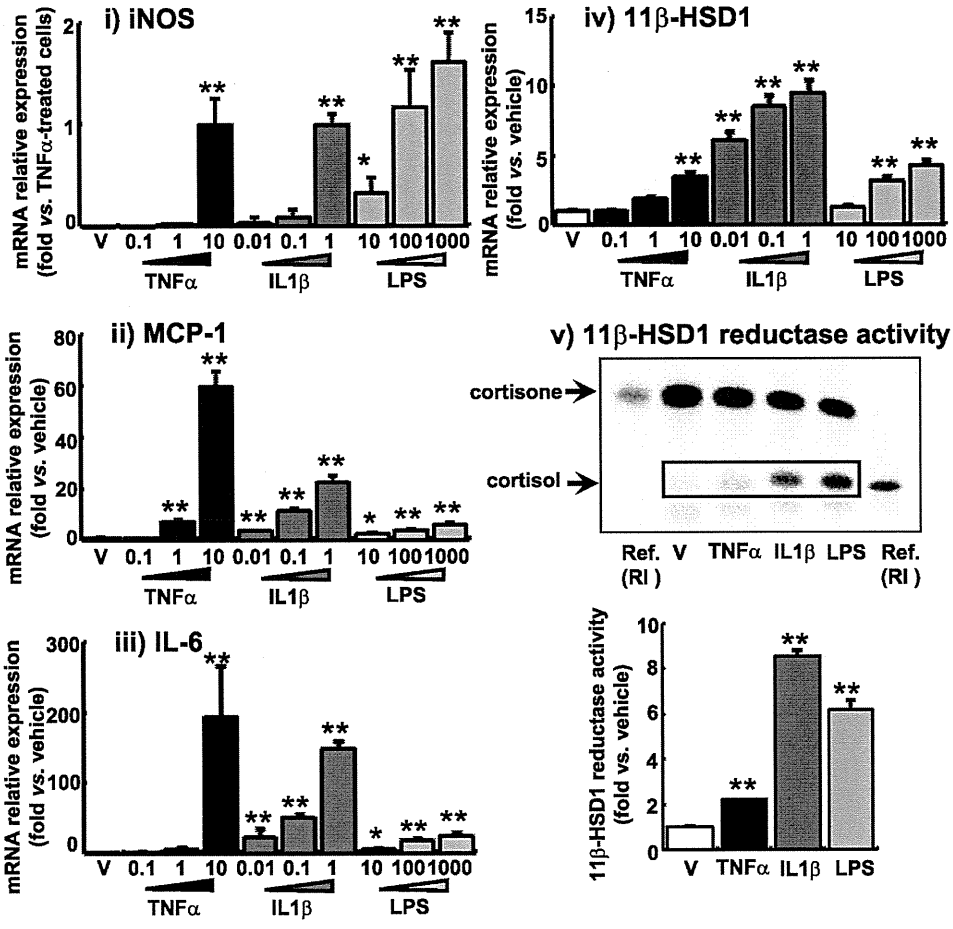

Fig. 2. TNF-α, IL-1β, and LPS augment the expression of proinflammatory mediators and 11β-HSD1 in 3T3-L1 preadipocytes. Cells were treated with TNF-α (0.1, 1, and 10 ng/ml), IL-1β, (0.01, 0.1, and 1 ng/ml) or LPS (10, 100, and 1,000 ng/ml) for 24 h. Levels of iNOS (*i*), MCP-1 (*ii*), IL-6 (*iii*), and 11β-HSD1 (*iv*) mRNA were quantified using real-time PCR. Values were normalized to that of 18S rRNA. *v*: 11β-HSD1 reductase activity (expressed as conversion ability of cortisone to cortisol) was assessed in the medium of 3T3-L1 cells treated with 10 ng/ml TNF-α, 1 ng/ml IL-1β, or 1,000 ng/ml LPS for 24 h. A reference of [^{3}H]cortisone or [^{3}H]cortisol was used as a size marker. A representative autoradiograph of thin-layer chromatography in 11β-HSD reductase activity assay (*top*) and quantification (*bottom*). Intensities of cortisol signals correspond to the enzyme activity of reductase. Ref. (RI), reference samples of [^{3}H]cortisone or [^{3}H]cortisol as size marker. Data are means ± SE of triplicate experiments. $^*P < 0.05$, $^{**}P < 0.01$, compared with vehicle (V)-treated group.

inhibitor, inhibitor A, has not been used for in vitro studies; however, another 11β-HSD1-specific inhibitor (compound 544) sharing almost the same structure as inhibitor A was used at a concentration of 5 μM (62). Therefore, in the present study, 10–50 μM CBX and 2.5–10 μM inhibitor A were used.

Before using these inhibitors in intact cells, we validated inhibitory potency of compounds against 11β-HSD1 in the microsome fraction assay. We verified that inhibitor A (10 nM) and CBX (1 μM) inhibited 11β-HSD1 activity as little as 25% vs. control, respectively, and that both of the 11β-HSD inhibitors suppressed 11β-HSD activity in a dose-dependent manner (Suppl. Fig. S2).

In 3T3-L1 preadipocytes, although CBX and inhibitor A did not change the level of 11β-HSD1 reductase activity, both of them suppressed TNF-α-induced reductase activity of 11β-HSD1 in a dose-dependent manner (Fig. 3*A*). CBX (50 μM) and inhibitor A (10 μM) markedly attenuated 11β-HSD1 activity (78 and 60% reduction vs. TNF-α-treated cells, respectively; Fig. 3*A*).

Without TNF-α-treatment, CBX and inhibitor A did not affect mRNA or protein levels of iNOS, MCP-1, and IL-6. On the other hand, in TNF-α-treated cells, these inhibitors reduced the mRNA and protein levels of proinflammatory genes. CBX decreased iNOS, MCP-1, and IL-6 mRNA levels (50 μM; iNOS: 83 ± 5%, MCP-1: 27 ± 4%, and IL-6: 47 ± 10% reduction vs. TNF-α-treated cells without compounds) and protein levels in the media (MCP-1: 17 ± 1% and IL-6: 34 ± 6% reduction) in TNF-α-treated 3T3-L1 preadipocytes (Fig. 3*B*). Similarly, inhibitor A reduced iNOS, MCP-1, and IL-6 mRNA (10 μM; iNOS: 47 ± 13%, MCP-1: 32 ± 12%, and IL-6: 33 ± 9% reduction) and protein levels in the media (MCP-1: 47 ± 3% and IL-6: 14 ± 3% reduction) (Fig. 3*C*).

Effect of 11β-HSD1 knockdown on proinflammatory properties in 3T3-L1 preadipocytes. To explore the potential role of 11β-HSD1 in cytokine release from activated preadipocytes, 11β-HSD1 was knocked down using siRNA. We tested four different siRNA sequences as described in MATERIALS AND METHODS; however, two of them did not suppress 11β-HSD1 mRNA level significantly in the preliminary experiments. Thus we demonstrated the data on si(1) and si(2).

When 3T3-L1 preadipocytes were transfected with 11β-HSD1 siRNA, TNF-α-induced expression of 11β-HSD1 was markedly attenuated [si(1): 60 ± 9% and si(2): 88 ± 7% reduction vs. negative control siRNA; Fig. 4*A*, *i*]. 11β-HSD1 reductase activity was also decreased by 11β-HSD1 siRNA [si(1): 81 ± 9% and si(2): 84 ± 3% reduction vs. negative control siRNA; Fig. 4*A*, *ii*]. 11β-HSD2 mRNA levels and the corresponding dehydrogenase activity were under detectable with or without siRNA treatments in 3T3-L1 preadipocytes (data not sown). Negative control RNAi did not influence the expression of 11β-HSD1. Knockdown of 11β-HSD1 in TNF-α-treated 3T3-L1 preadipocytes effectively reduced iNOS, MCP-1, and IL-6 mRNA levels [si(1): IL-6: 32 ± 7% reduction; and si(2): iNOS: 37 ± 8%, MCP-1: 22 ± 5%, and IL-6: 59 ± 3% reduction] and protein levels in the media [si(1):

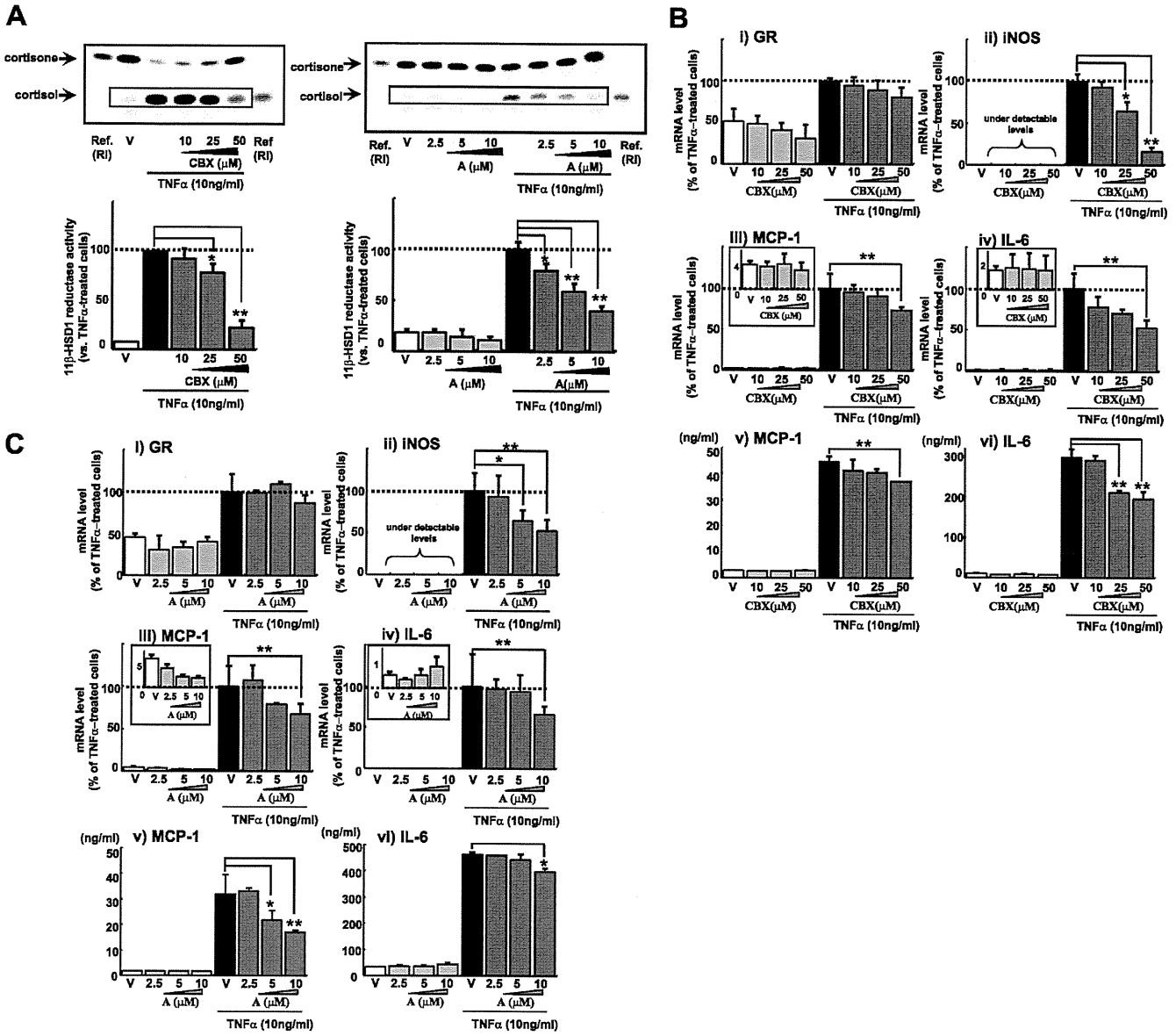

Fig. 3. Effects of pharmacological inhibition of 11β-HSD1 on glucocorticoid receptor (GR), MCP-1, IL-6, and iNOS expression in and secretion from TNF-α-treated 3T3-L1 preadipocytes. *A*: 11β-HSD1 activity assay for validation of 11β-HSD1 inhibitors. 3T3-L1 preadipocytes were incubated for 24 h in serum-free DMEM, adding 250 nM of cortisone with tritium-labeled cortisone. A representative autoradiograph of TLC for the 11β-HSD1 activity assay (*top*) and quantification of 11β-HSD1 activities (*bottom*). Intensities of cortisol signals correspond to the reductase activity. The *y*-axis shows percent 11β-HSD1 reductase activity compared with TNF-α (10 mg/ml)-treated cells. carbenoxolone (CBX; 10–50 μM) and inhibitor A (A; 2.5–10 μM) substantially reduced 11β-HSD1 activity in 3T3-L1 preadipocytes. CBX (*B*; 10–50 μM) and inhibitor A (*C*; 2.5–10 μM) 3T3-L1 preadipocytes were treated with TNF-α (10 ng/ml) or cotreated with CBX and inhibitor A for 24 h. GR (*i*), iNOS (*ii*), MCP-1 (*iii*), and IL-6 (*iv*) mRNA levels were determined using real-time PCR. Values were normalized to that of 18S rRNA and expressed relative to TNF-α-treated cells. Concentrations of MCP-1 (*v*) and IL-6 (*vi*) in the medium were measured with ELISA. Data are means ± SE of triplicate experiments. $*P < 0.05$, $** P < 0.01$, compared with TNF-α-treated cells.

MCP-1: 13 ± 1% and IL-6: 17 ± 1% reduction; and si(2): MCP1: 19 ± 7% and IL-6: 30 ± 1% reduction; Fig. 4*B*].

Overexpression of 11β-HSD1 augmented iNOS, MCP-1, and IL-6 in TNF-α-treated 3T3-L1 preadipocytes. We examined whether overexpression of 11β-HSD1 is relevant to the augmentation of proinflammatory molecules in activated preadipocytes. The extent of 11β-HSD1 overexpression in 3T3-L1 preadipocytes was assessed by 11β-HSD1 mRNA levels and reductase activity (Fig. 5*A*). As expected, 11β-HSD1 mRNA level was increased by treatment of the 11β-HSD1 vector (~20-fold) or 10 ng/ml TNF-α (~300-fold) compared with the vehicle. TNF-α-induced expression of 11β-HSD1 was further augmented by the introduction of the 11β-HSD1 vector (1.6-fold vs. empty vector). Reductase activity of 11β-HSD1 was also increased by the introduction of the vector (2-fold) or 10 ng/ml TNF-α (10-fold). Notably, TNF-α-induced enzyme activity was further augmented by the vector (1.3-fold vs. empty vector).

Expression of iNOS, MCP-1, and IL-6 did not differ between the 11β-HSD1 vector and the empty vector. On the other hand, TNF-α-induced expression of iNOS, MCP-1, and IL-6 was augmented in 11β-HSD1 transfectants (MCP-1: 172 ±

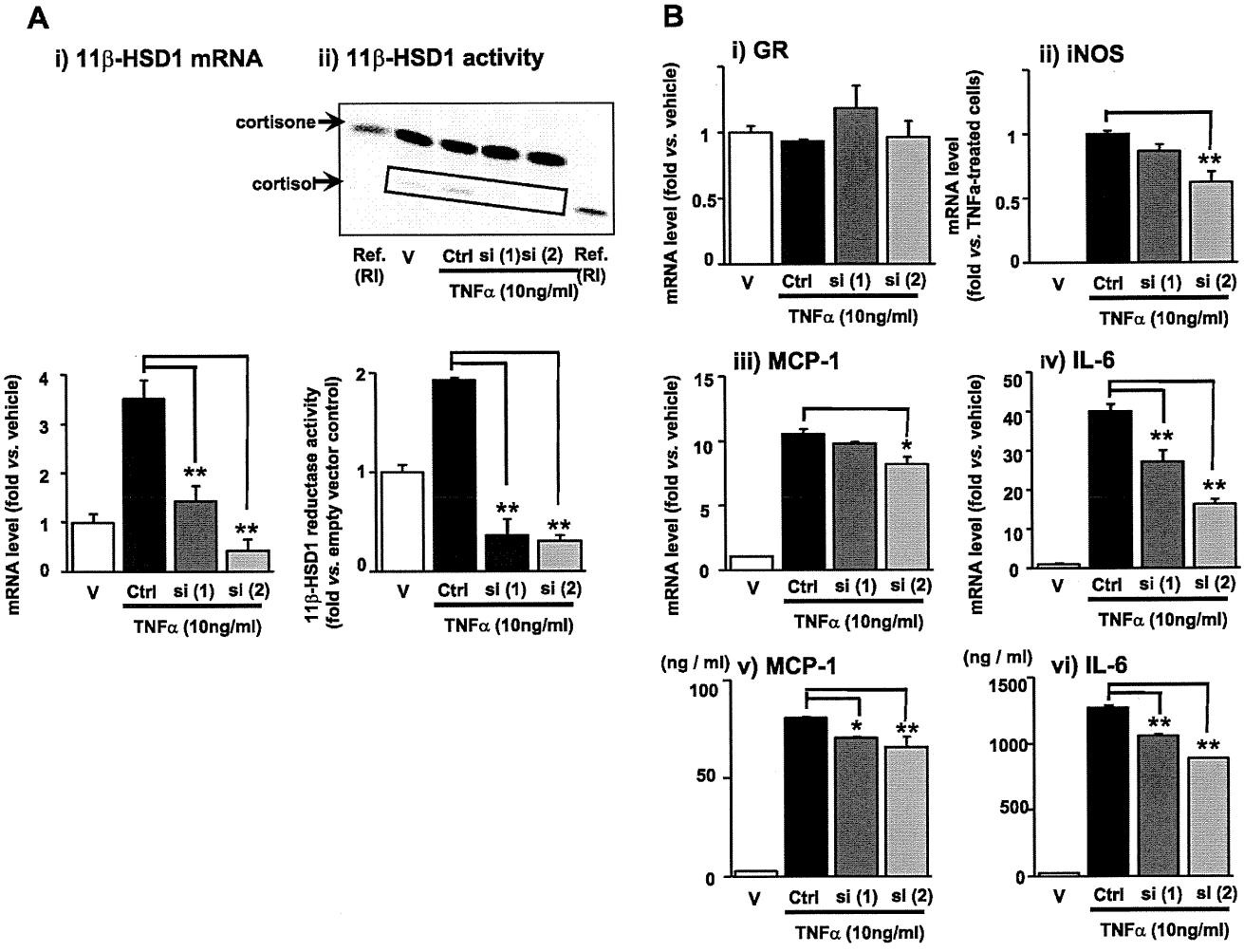

Fig. 4. Effects of 11β-HSD1 knockdown on TNF-α-induced expression of 11β-HSD1 in 3T3-L1 preadipocytes. Cells were transfected with either RNA interference for mouse 11β-HSD1 or a negative control (Ctrl). After 12 h incubation, cells were treated with 10 ng/ml TNF-α for 24 h. *A*: efficiency of 11β-HSD1 knockdown by small-interfering RNA. 11β-HSD1 mRNA (*i*) and reductase activity (*ii*). *B*: effects of knockdown of 11β-HSD1 on MCP-1, IL-6, and iNOS expression in and secretion from TNFα-treated 3T3-L1 preadipocytes. 11β-HSD1 (*i*), GR (*ii*), iNOS (*iii*), MCP-1 (*iv*), and IL-6 mRNA (*v*) levels were determined using real-time PCR. Values were normalized to that of 18S rRNA and expressed as a relative level vs. vehicle control (V). Concentrations of MCP-1 (*vi*) and IL-6 (*vii*) in the medium were measured with ELISA. Data are means ± SE of triplicate experiments. $^*P < 0.05$, $^{**}P < 0.01$, compared with TNF-α-treated cells. siRNA for mouse 11β-HSD1: si(1): MSS205244 (Invitrogen) and si(2): sense: 5′-GAAAUGGCAUAUCAUCUGUTT-3′ and antisense: 3′-TTCUUUACCGUAUAGUAGACA-5′ (Takara).

88%, IL-6: 194 ± 64%, and iNOS: 187 ± 47% vs. the empty vector; Fig. 5*B*, *ii-iv*). Similarly, protein levels of MCP-1 and IL-6 in the media were increased in transfectants (MCP-1: 206 ± 32% and IL-6: 156 ± 17% vs. the empty vector; Fig. 5*B*, *v* and *vi*).

Pharmacological inhibition of 11β-HSD1 attenuated TNF-α-induced NF-κB and MAPK signaling in 3T3-L1 preadipocytes. We examined the possible involvement of 11β-HSD1 in proinflammatory signaling pathways. 3T3-L1 preadipocytes were incubated with TNF-α (10 ng/ml), with or without CBX (50 μM) and inhibitor A (10 μM) for 24 h. After a 2-h serum starvation, the cells were incubated with TNF-α (10 ng/ml), with or without CBX (50 μM) and inhibitor A (10 μM) for 10 min. TNF-α-induced p-65 phosphorylation was markedly attenuated by CBX (30 ± 12% decrease vs. TNF-α-treated cells) and inhibitor A (51 ± 11% decrease vs. TNF-α-treated cells; Fig. 6*A*). Regarding MAPK signaling, augmented phosphorylation of p-38, JNK, and ERK with the TNF-α treatment was substantially attenuated by CBX (p-38: 26 ± 8% decrease and JNK: 48 ± 3% decrease vs. TNF-α-treated cells) and inhibitor A (p-38: 51 ± 9% decrease, JNK: 72 ± 5% decrease, and ERK: 36 ± 11% decrease vs. TNF-α-treated cells; Fig. 6*B*).

Pharmacological inhibition of 11β-HSD1 attenuated iNOS, MCP-1, and IL-6 mRNA levels in SVF cells from ob/ob mice. We examined the effects of pharmacological inhibition of 11β-HSD1 on proinflammatory gene expression in primary cultured SVF cells isolated from epididymal fat depots in obese *ob/ob* mice or lean control mice.

CBX (50 μM) and inhibitor A (10 μM) did not change the expression level of 11β-HSD1 (Fig. 7*i*). CBX decreased mRNA level of iNOS, MCP-1, and IL-6 in both the basal state (iNOS: 69 ± 4%, MCP1: 42 ± 7%, and IL-6: 56 ± 14% reduction vs. vehicle control) and TNFα-stimulated state (iNOS: 58 ± 11%, MCP-1: 63 ± 5%, and IL-6: 53 ± 8% reduction vs. TNFα-treated cells without compounds) in SVF cells from *ob/ob* mice.

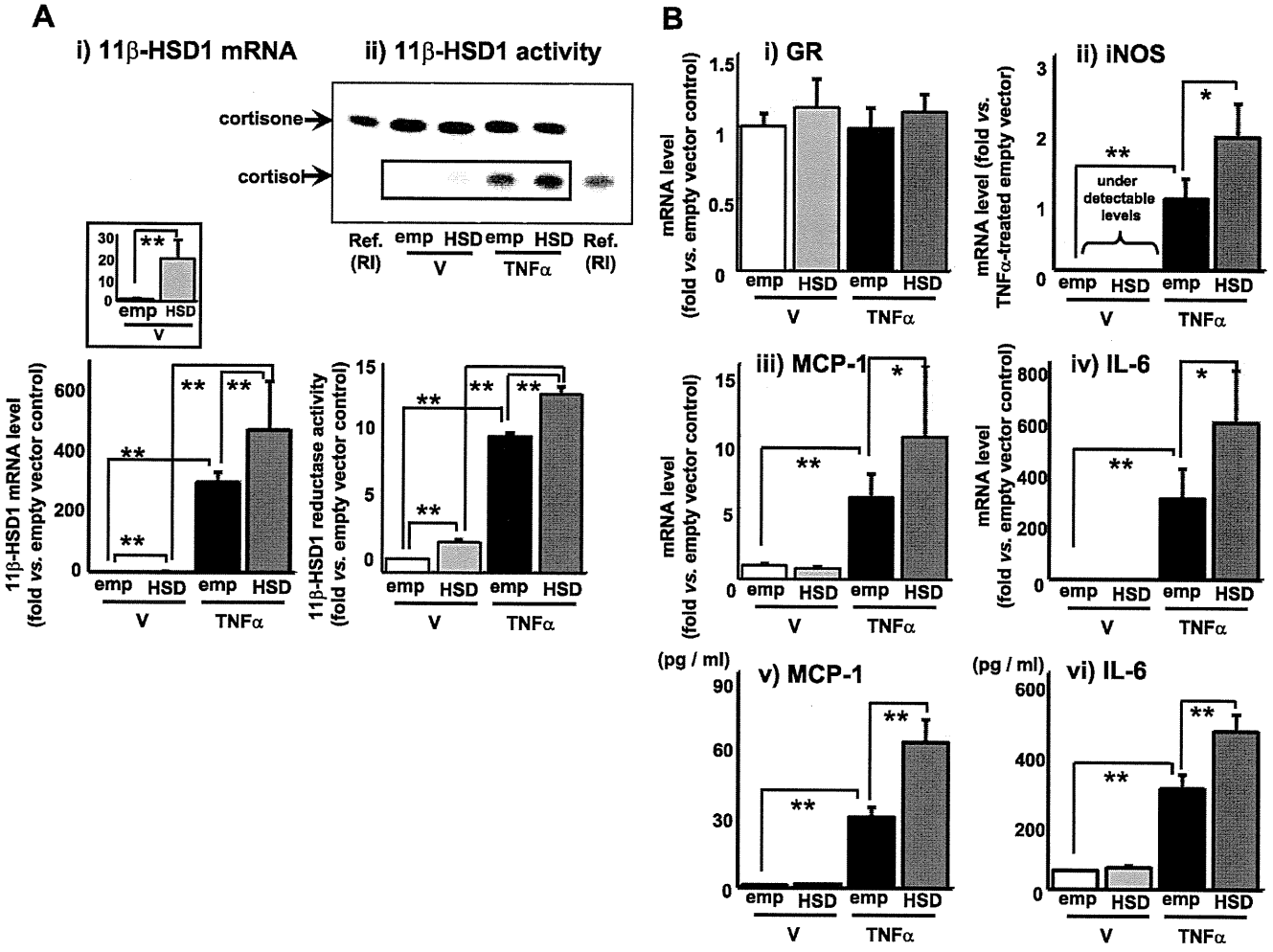

Fig. 5. Effects of overexpression of 11β-HSD1 on MCP-1, IL-6, and iNOS expression in and secretion from TNF-α-treated 3T3-L1 preadipocytes. *A*: efficiency of electroporation-mediated gene transfer. 3T3-L1 preadipocytes were transfected with the expression vector for 11β-HSD1 or a corresponding empty vector using electroporation. After 48 h, cells were treated with or without 10 ng/ml TNF-α for 24 h. Cells were assayed for 11β-HSD1 mRNA (*i*) and reductase activity (*ii*). *B*: effects of overexpression of 11β-HSD1 on MCP-1, IL-6, and iNOS expression in and secretion from TNF-α-treated 3T3-L1 preadipocytes. 3T3-L1 preadipocytes were transfected as above, and 48 h after the infection, cells were treated with or without 10 ng/ml TNF-α for 24 h. Levels of mRNA for GR (*i*), iNOS (*ii*), MCP-1 (*iii*), and IL-6 (*iv*) were determined using real-time PCR. Values were normalized to those of 18S rRNA and expressed as a relative level vs. the vehicle control (V). Concentrations of MCP-1 (*v*) and IL-6 (*vi*) in the medium were measured with ELISA. Data are means ± SE of triplicate experiments. $^{*}P < 0.05$, $^{**}P < 0.01$.

Without TNF-α-treatment, CBX did not change mRNA levels of iNOS, MCP-1 and IL-6 in SVF cells from lean control mice. However, CBX reduced the mRNA levels of iNOS, MCP-1, and IL-6 (iNOS: 64 ± 18%, MCP-1: 67 ± 14%, and IL-6: 58 ± 12% reduction vs. TNF-α-treated cells without compounds) in TNF-α-treated SVF cells from lean control mice (Fig. 7).

Pharmacological inhibition of 11β-HSD1 attenuated NF-κB and MAPK signaling in SVF cells from ob/ob mice. SVF cells from *ob/ob* or lean control mice were incubated with TNF-α (10 ng/ml), with or without CBX (50 μM) and inhibitor A (10 μM) for 24 h. After a 2-h serum starvation, the cells were incubated with TNF-α (10 ng/ml), with or without CBX (50 μM) and inhibitor A (10 μM) for 10 min. Activation of NF-κB (p65) and MAPK (p38, JNK, and ERK) signaling did occur in SVF cells from *ob/ob* mice compared with lean control (Suppl. Fig. S3). In *ob/ob* mice, phosphorylation of these signaling without TNF-α treatment was attenuated by CBX and inhibitor A. TNF-α-induced p-65, p38, JNK, and ERK phosphorylation was also attenuated by CBX and inhibitor A in SVF cells from both *ob/ob* and lean control mice (Suppl. Fig. S3).

DISCUSSION

Here we provide novel evidence that inflammatory stimuli-induced 11β-HSD1 in activated preadipocytes intensifies NF-κB and MAPK signaling pathways and the resultant augmentation of proinflammatory molecules. Not limited to 3T3-L1 preadipocytes, we also demonstrated the notion was reproducible in the primary SVF cells from obese mice. Previous works focused on the metabolically beneficial impact of 11β-HSD1 deficiency on adipose tissue distribution, fuel homeostasis, and insulin sensitivity. On the other hand, clearly distinct from previous works, our present study is the first to highlight an unexpected, proinflammatory role of reamplified glucocorticoids within activated preadipocytes in obese adipose tissue.

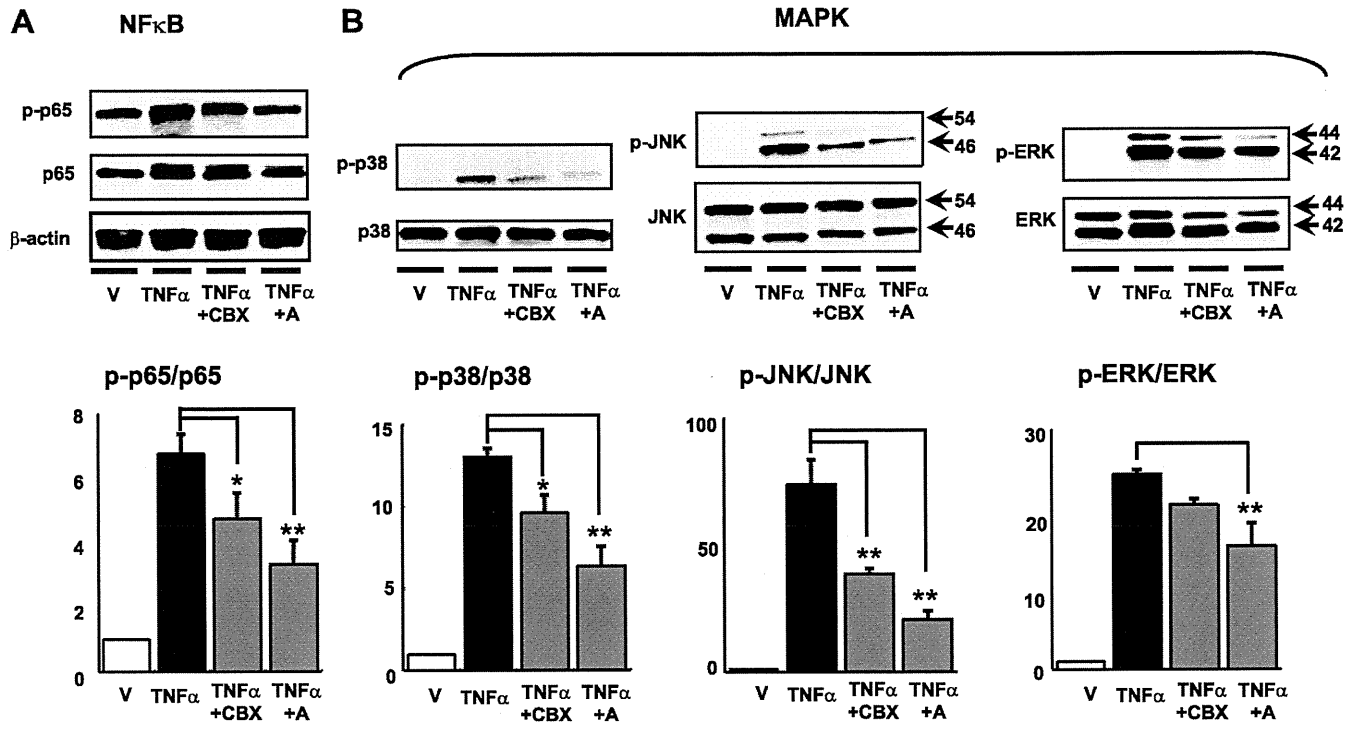

Fig. 6. Effects of inhibition of 11β-HSD1 on TNF-α-induced NFκB and MAPK signaling. NFκB (*A*) and MAPK (*B*) signaling pathways. 3T3-L1 preadipocytes were treated with 10 ng/ml TNF-α for 24 h in the presence or absence of 11β-HSD1 inhibitors (CBX or inhibitor A). After 2-h serum starvation, cells were treated with TNF-α in the presence or absence of 11β-HSD1 inhibitors for 10 min to assess the activation of NFκB and MAPK signaling pathways. Western blot analyses were performed using antibodies against β-actin and NFkB-p65 (*A*), phospho-p65 (*B*), p38-MAPK (*B, left*), phospho-p38 (*B, center*) JNK, phospho-JNK (*B, right*) ERK 1/2, and phospho-ERK1/2. A representative Western blot (*top*) and quantification of p65, p38, JNK, and ERK phosphorylation (*bottom*). Data are means ± SE of triplicate experiments. $*P < 0.05$, $**P < 0.01$ compared with TNF-α-treated cells.

Suppression and overexpression experiments with 11β-HSD1 in activated preadipocytes demonstrate that TNF-α-induced 11β-HSD1 further augments the expression of proinflammatory genes including iNOS, MCP-1, and IL-6. Elevation of iNOS, MCP-1, and IL-6 in adipose tissue is commonly observed in obese subjects, linking to dysfunction of adipose tissue (19, 29, 45, 56). For example, iNOS-deficient mice are protected against obesity-induced insulin resistance and glucose intolerance (45). Moreover, transgenic mice overexpressing MCP-1 in adipose tissue exemplify insulin resistance and exaggerated infiltration of macrophages into adipose tissue (29). Previous studies (20, 36) showed that adipose tissue is a primary production site for IL-6 in humans. In fact, circulating IL-6 levels are shown to elevate in patients with insulin-resistance (19, 56), impaired glucose tolerance (40), and type 2 diabetes (47). Taken together, the present study provides novel evidence for proinflammatory role of 11β-HSD1 in activated preadipocytes.

To optimize experimental condition, the present study was designed to eliminate possible toxic effects and nonspecific effects of 11β-HSD1 inhibitors. Because 11β-HSD2 mRNA and corresponding dehydrogenase enzyme activity (8, 27) were undetected in 3T3-L1 preadipocytes even after the treatment with TNF-α (unpublished observations), CBX virtually serves as a specific inhibitor against 11β-HSD1 in the present study. To further verify the effect of 11β-HSD1 inhibition on activated preadipocytes, we confirmed that an 11β-HSD1-specific inhibitor A exerted similar effects to CBX (Fig. 3). Of note, the expression level of the glucocorticoid receptor did not vary by the treatment with 11β-HSD1 inhibitors (unpublished observations). The notion that TNF-α-induced 11β-HSD1 would reinforce the expression of proinflammatory genes was endorsed by the results of RNAi experiments (Fig. 4) and overexpression experiments (Fig. 5). It should be emphasized that forced overexpression of 11β-HSD1 per se did not influence the expression level of proinflammatory genes in nonactivated preadipocytes (Fig. 5*B*). These findings led us to speculate that 11β-HSD1-mediated active glucoorticoids within cells reinforce inflammation under proinflammatory conditions commonly seen in obese adipose tissue.

The present study demonstrated that 11β-HSD1 was highly expressed in SVF cells from obese adipose tissue (Fig. 1). Although mature adipocytes abundantly express 11β-HSD1 (44, 61), a considerable amount of 11β-HSD1 expression was detected in SVF from adipose tissue (Fig. 1). Potential link between preadipocyte function and pathophysiology of obese adipose tissue has recently attracted research interest (53, 57). A recent study (14) using 11β-HSD1 knockout mice provided evidence that 11β-HSD1 in preadipocytes may affect fat distribution under overnutrition. In 3T3-L1 cells, the expression level of 11β-HSD1 is lower in preadipocytes but is dramatically increased during the course of differentiation into mature adipocytes (51). In fact, active glucocorticoids generated intracellularly by 11β-HSD1 are critical for normal adipose differentiation (33). On the other hand, TNF-α augments 11β-HSD1 expression in preadipocytes (Fig. 2). Of note, in proinflammatory milieu, TNF-α inhibits adipocyte differentiation by decreasing PPARγ expression (43, 46, 64). Depending on the

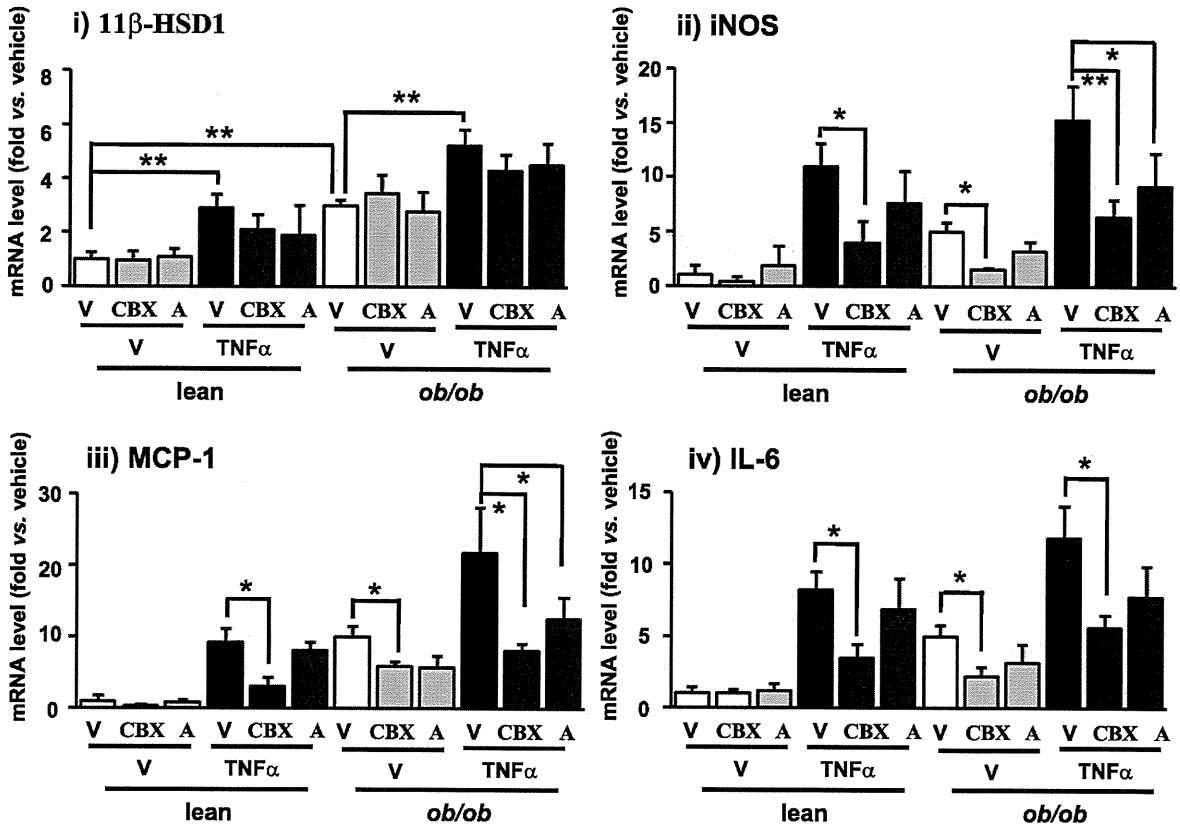

Fig. 7. Effects of pharmacological inhibition of 11β-HSD1 on iNOS, MCP-1, and IL-6 mRNA levels in SVF cells from *ob/ob* mice. SVF cells from *ob/ob* mice and lean control mice were treated with CBX (50 μM) or inhibitor A (10 μM), with or without TNF-α (10 ng/ml) for 24 h. 11β-HSD1 (*i*), iNOS (*ii*), MCP-1 (*iii*), and IL-6 mRNA (*iv*) levels were determined using real-time PCR. Values were normalized to that of 18S rRNA and expressed relative to lean control. Data are means ± SE of triplicate experiments. $^{*}P < 0.05$, $^{**}P < 0.01$.

hormonal milieu, it is therefore conceivable that 11β-HSD1 plays a role in both adipogenesis and inflammatory response in preadipoytes.

We assessed the expression of Pref-1 (a representative molecular marker for preadipocytes; Ref. 7) as well as aP2, PPARγ2, and GLUT4 (a set of representative markers for differentiated adipocytes; Refs. 32 and 59) in preadipocytes overexpressing 11β-HSD1. Consequently, forced augmentation of 11β-HSD1 did not affect the expression level of these genes (Suppl. Fig. S4), supporting that a line of our observation was not a facet of mature adipocytes but of preadipocytes.

Previous studies demonstrated that chronic inflammation is closely associated with insulin resistance in insulin-sensitive organs (24, 64). Glucocorticoids are widely used as anti-inflammatory agents in a clinical setting (49). On the other hand, this hormone simultaneously causes insulin resistance (4, 50). Regarding this apparent paradox, recent studies (34, 55) suggest that reactivated glucocorticoids within cells have the potential to enhance inflammatory or immune responses in a variety of cells. In the present study, replenished dexamethasone in the culture media at pharmacological doses did decrease the synthesis and secretion of proinflammatory molecules in preadipocytes in a dose-dependent manner (Fig. 3). On the other hand, in activated preadipocytes, 11β-HSD1 intensifies TNF-α-induced activation of NF-κB and the MAPK signaling cascade (Fig. 6). In this context, it is possible that intracellular activation of glucocorticoids within physiological range would likely cause proinflammatory responses in certain cell types. It should be noted that preadipocytes possess very few insulin receptors (51). Instead, preadipocytes express a large number of IGF-1 receptors (18). Insulin can bind to the IGF-1 receptor only at supraphysiological concentrations. However, it is likely that increased release of inflammatory cytokines from activated preadipocytes may aggravate insulin receptor signaling in adjacent mature adipocytes in obese adipose tissue. This notion is supported by a line of mouse experiments showing that pharmacological inhibition of 11β-HSD1 ameliorated diabetes, dyslipidemia, and even arteriosclerosis (1, 23).

PPARγ agonists potently suppress the activity of 11β-HSD1 exclusively in adipose tissue (6). The present finding that amplified glucocorticoids within activated preadipocytes may enhance inflammatory responses does not contradict the notion that PPARγ agonists exert potent anti-inflammatory effects in a variety of cell types (37).

Recent studies showed that phosphoinositide 3-kinase (PI3K)-Akt pathways, IL-1 receptor-associated kinase-M (IRAK-M), and suppressors of cytokine signaling-1 (SOCS-1) are negative regulators of NF-κB and MAPK signaling (21). Under inflammatory stimuli, a physiological dose of glucocorticoids positively regulates the expression of SHIP1, a phosphatase that negatively regulates PI3K signaling, resulting in the activation of NF-κB and MAPK in activated macrophages (67). Considering the close biological similarities between activated preadipocytes and activated macrophages (11, 13), we explored whether PI3K-Akt pathways, SHIP1, or other phosphatases could be

involved in the 11β-HSD1-induced NF-κB and MAPK activation. Western blot analyses indicated that phosphorylation of Akt or protein levels of SHIP1, PP2A, or MKP-1 did not change significantly with inhibition or overexpression of 11β-HSD1 (Suppl. Fig. S5). Further studies are warranted to unravel the entire mechanism.

In summary, the present study provides novel evidence that inflammatory stimuli-induced 11β-HSD1 reinforces NF-κB and MAPK signaling pathways and results in further induction of proinflammatory molecules in activated preadipocytes. Our findings highlight an unexpected, inflammatory role of reactivated glucocorticoids within preadipocytes in obese adipose tissue.

ACKNOWLEDGMENTS

We thank A. Ryu, S. Maki, M. Nagamoto, T. Fukui, Y. Kobayashi, S. Yamauchi, and K. Takahashi for assistance.

GRANTS

This work was supported in part by a Grant-in-Aid for Scientific Research (B2:19390248), the Takeda Medical Research Foundation, and the Lilly Research Foundation.

DISCLOSURES

No conflicts of interest are declared by the author(s).

REFERENCES

1. **Alberts P, Nilsson C, Selen G, Engblom LO, Edling NH, Norling S, Klingstrom G, Larsson C, Forsgren M, Ashkzari M, Nilsson CE, Fiedler M, Bergqvist E, Ohman B, Bjorkstrand E, Abrahmsen LB.** Selective inhibition of 11 beta-hydroxysteroid dehydrogenase type 1 improves hepatic insulin sensitivity in hyperglycemic mice strains. *Endocrinology* 144: 4755–4762, 2003.
2. **Andrew R, Phillips DI, Walker BR.** Obesity and gender influence cortisol secretion and metabolism in man. *J Clin Endocrinol Metab* 83: 1806–1809. 1998.
3. **Andrews RC, Rooyackers O, Walker BR.** Effects of the 11 beta-hydroxysteroid dehydrogenase inhibitor carbenoxolone on insulin sensitivity in men with type 2 diabetes. *J Clin Endocrinol Metab* 88: 285–291, 2003.
4. **Asensio C, Muzzin P, Rohner-Jeanrenaud F.** Role of glucocorticoids in the physiopathology of excessive fat deposition and insulin resistance. *Int J Obes Relat Metab Disord* 28 *Suppl* 4: S45–52, 2004.
5. **Balachandran A, Guan H, Sellan M, van Uum S, Yang K.** Insulin and dexamethasone dynamically regulate adipocyte 11beta-hydroxysteroid dehydrogenase type 1. *Endocrinology* 149: 4069–4079, 2008.
6. **Berger J, Tanen M, Elbrecht A, Hermanowski-Vosatka A, Moller DE, Wright SD, Thieringer R.** Peroxisome proliferator-activated receptor-gamma ligands inhibit adipocyte 11beta-hydroxysteroid dehydrogenase type 1 expression and activity. *J Biol Chem* 276: 12629–12635, 2001.
7. **Boney CM, Fiedorek FT Jr, Paul SR, Gruppuso PA.** Regulation of preadipocyte factor-1 gene expression during 3T3–L1 cell differentiation. *Endocrinology* 137: 2923–2928, 1996
8. **Bujalska IJ, Kumar S, Stewart PM.** Does central obesity reflect "Cushing's disease of the omentum"? *Lancet* 349: 1210–1213, 1997.
9. **Cancello R, Henegar C, Viguerie N, Taleb S, Poitou C, Rouault C, Coupaye M, Pelloux V, Hugol D, Bouillot JL, Bouloumie A, Barbatelli G, Cinti S, Svensson PA, Barsh GS, Zucker JD, Basdevant A, Langin D, Clement K.** Reduction of macrophage infiltration and chemoattractant gene expression changes in white adipose tissue of morbidly obese subjects after surgery-induced weight loss. *Diabetes* 54: 2277–2286, 2005.
10. **Chapman KE, Coutinho AE, Gray M, Gilmour JS, Savill JS, Seckl JR.** The role and regulation of 11beta-hydroxysteroid dehydrogenase type 1 in the inflammatory response. *Mol Cell Endocrinol* 301: 123–131, 2009.
11. **Charriere G, Cousin B, Arnaud E, Andre M, Bacou F, Penicaud L, Casteilla L.** Preadipocyte conversion to macrophage. Evidence of plasticity. *J Biol Chem* 278: 9850–9855, 2003.
12. **Chung S, Lapoint K, Martinez K, Kennedy A, Boysen Sandberg M, McIntosh MK.** Preadipocytes mediate lipopolysaccharide-induced inflammation and insulin resistance in primary cultures of newly differentiated human adipocytes. *Endocrinology* 147: 5340–5351, 2006.
13. **Cousin B, Munoz O, Andre M, Fontanilles AM, Dani C, Cousin JL, Laharrague P, Casteilla L, Penicaud L.** A role for preadipocytes as macrophage-like cells. *FASEB J* 13: 305–312, 1999.
14. **De Sousa Peixoto RA, Turban S, Battle JH, Chapman KE, Seckl JR, Morton NM.** Preadipocyte 11beta-hydroxysteroid dehydrogenase type 1 is a keto-reductase and contributes to diet-induced visceral obesity in vivo. *Endocrinology* 149: 1861–1868, 2008.
16. **Dembinska-Kiec A, Pallapies D, Simmet T, Peskar BM, Peskar BA.** Effect of carbenoxolone on the biological activity of nitric oxide: relation to gastroprotection. *Br J Pharmacol* 104: 811–816, 1991.
17. **Elsen FP, Shields EJ, Roe MT, Vandam RJ, Kelty JD.** Carbenoxolone induced depression of rhythmogenesis in the pre-Botzinger complex. *BMC Neurosci* 9: 46, 2008.
18. **Entingh-Pearsall A, Kahn, CR.** Differential roles of the insulin and insulin-like growth factor-i (igf-i) receptors in response to insulin and IGF-I. *J Biol Chem* 279: 38016–38024, 2004.
19. **Fernandez-Real JM, Vayreda M, Richart C, Gutierrez C, Broch M, Vendrell J, Ricart W.** Circulating interleukin 6 levels, blood pressure, and insulin sensitivity in apparently healthy men and women. *J Clin Endocrinol Metab* 86: 1154–1159, 2001.
20. **Fried SK, Bunkin DA, Greenberg AS.** Omental and subcutaneous adipose tissues of obese subjects release interleukin-6: depot difference and regulation by glucocorticoid. *J Clin Endocrinol Metab* 83: 847–850, 1998.
21. **Fukao T, Koyasu S.** PI3K and negative regulation of TLR signaling. *Trends Immunol* 24: 358–363, 2003.
22. **Hauner H.** Secretory factors from human adipose tissue and their functional role. *Proc Nutr Soc* 64: 163–169, 2005.
23. **Hermanowski-Vosatka A, Balkovec JM, Cheng K, Chen HY, Hernandez M, Koo GC, Le Grand CB, Li Z, Metzger JM, Mundt SS, Noonan H, Nunes CN, Olson SH, Pikounis B, Ren N, Robertson N, Schaeffer JM, Shah K, Springer MS, Strack AM, Strowski M, Wu K, Wu T, Xiao J, Zhang BB, Wright SD, Thieringer R.** 11beta-HSD1 inhibition ameliorates metabolic syndrome and prevents progression of atherosclerosis in mice. *J Exp Med* 202: 517–527, 2005.
24. **Hotamisligil GS.** Inflammation and metabolic disorders. *Nature* 444: 860–867, 2006.
25. **Hult M, Shafqat N, Elleby B, Mitschke D, Svensson S, Forsgren M, Barf T, Vallgarda J, Abrahmsen L, Oppermann U.** Active site variability of type 1 11beta-hydroxysteroid dehydrogenase revealed by selective inhibitors and cross-species comparisons. *Mol Cell Endocrinol* 248: 26–33, 2006.
26. **Ishii T, Masuzaki H, Tanaka T, Arai N, Yasue S, Kobayashi N, Tomita T, Noguchi M, Fujikura J, Ebihara K, Hosoda K, Nakao K.** Augmentation of 11beta-hydroxysteroid dehydrogenase type 1 in LPS-activated J774.1 macrophages–role of 11beta-HSD1 in pro-inflammatory properties in macrophages. *FEBS Lett* 581: 349–354, 2007.
27. **Jamieson PM, Chapman KE, Edwards CR, Seckl JR.** 11 beta-hydroxysteroid dehydrogenase is an exclusive 11 beta- reductase in primary cultures of rat hepatocytes: effect of physicochemical and hormonal manipulations. *Endocrinology* 136: 4754–4761, 1995.
28. **Julien P, Despres JP, Angel A.** Scanning electron microscopy of very small fat cells and mature fat cells in human obesity. *J Lipid Res* 30: 293–299, 1989.
29. **Kanda H, Tateya S, Tamori Y, Kotani K, Hiasa K, Kitazawa R, Kitazawa S, Miyachi H, Maeda S, Egashira K, Kasuga M.** MCP-1 contributes to macrophage infiltration into adipose tissue, insulin resistance, and hepatic steatosis in obesity. *J Clin Invest* 116: 1494–1505, 2006.
30. **Kershaw EE, Morton NM, Dhillon H, Ramage L, Seckl JR, Flier JS.** Adipocyte-specific glucocorticoid inactivation protects against diet-induced obesity. *Diabetes* 54: 1023–1031, 2005.
31. **Kotelevtsev Y, Holmes MC, Burchell A, Houston PM, Schmoll D, Jamieson P, Best R, Brown R, Edwards CR, Seckl JR, Mullins JJ.** 11beta-hydroxysteroid dehydrogenase type 1 knockout mice show attenuated glucocorticoid-inducible responses and resist hyperglycemia on obesity or stress. *Proc Natl Acad Sci USA* 94: 14924–14929, 1997.
32. **Lane MD, Tang QQ, Jiang MS.** Role of the CCAAT enhancer binding proteins (C/EBPs) in adipocyte differentiation. *Biochem Biophys Res Commun* 266: 677–683, 1999.

33. **Liu Y, Sun Y, Zhu T, Xie Y, Yu J, Sun WL, Ding GX, Hu G.** 11β HSD1 promotes differentiation of 3T3-L1 preadipocyte. *Acta Pharmacol Sin* 28: 1198–204, 2007.
34. **McEwen BS, Biron CA, Brunson KW, Bulloch K, Chambers WH, Dhabhar FS, Goldfarb RH, Kitson RP, Miller AH, Spencer RL, Weiss JM.** The role of adrenocorticoids as modulators of immune function in health and disease: neural, endocrine and immune interactions. *Brain Res Brain Res Rev* 23: 79–133, 1997.
35. **McLaughlin T, Sherman A, Tsao P, Gonzalez O, Yee G, Lamendola C, Reaven GM, Cushman SW.** Enhanced proportion of small adipose cells in insulin-resistant vs insulin-sensitive obese individuals implicates impaired adipogenesis. *Diabetologia* 50: 1707–1715, 2007.
36. **Mohamed-Ali V, Goodrick S, Rawesh A, Katz DR, Miles JM, Yudkin JS, Klein S, Coppack SW.** Subcutaneous adipose tissue releases interleukin-6, but not tumor necrosis factor-alpha, in vivo. *J Clin Endocrinol Metab* 82: 4196–4200, 1997.
37. **Moller DE, Berger JP.** Role of PPARs in the regulation of obesity-related insulin sensitivity and inflammation. *Int J Obes Relat Metab Disord* 27 *Suppl* 3: S17–21, 2003.
38. **Montague CT, O'Rahilly S.** The perils of portliness: causes and consequences of visceral adiposity. *Diabetes* 49: 883–888, 2000.
39. **Morton NM, Paterson JM, Masuzaki H, Holmes MC, Staels B, Fievet C, Walker BR, Flier JS, Mullins JJ, Seckl JR.** Novel adipose tissue-mediated resistance to diet-induced visceral obesity in 11β-hydroxysteroid dehydrogenase type 1-deficient mice. *Diabetes* 53: 931–938, 2004.
40. **Muller S, Martin S, Koenig W, Hanifi-Moghaddam P, Rathmann W, Haastert B, Giani G, Illig T, Thorand B, Kolb H.** Impaired glucose tolerance is associated with increased serum concentrations of interleukin 6 and co-regulated acute-phase proteins but not TNF-alpha or its receptors. *Diabetologia* 45: 805–812, 2002.
41. **Napolitano A, Voice MW, Edwards CR, Seckl JR, Chapman KE.** 11beta-hydroxysteroid dehydrogenase 1 in adipocytes: expression is differentiation-dependent and hormonally regulated. *J Steroid Biochem Mol Biol* 64: 251–260, 1998.
42. **Ohara Y, Peterson TE, Harrison DG.** Hypercholesterolemia increases endothelial superoxide anion production. *J Clin Invest* 91: 2546–2551, 1993.
43. **Pape ME, Kim KH.** Effect of tumor necrosis factor on acetyl-coenzyme A carboxylase gene expression and preadipocyte differentiation. *Mol Endocrinol* 2: 395–403, 1988.
44. **Paulmyer-Lacroix O, Boullu S, Oliver C, Alessi MC, Grino M.** Expression of the mRNA coding for 11beta-hydroxysteroid dehydrogenase type 1 in adipose tissue from obese patients: an in situ hybridization study. *J Clin Endocrinol Metab* 87: 2701–2705, 2002.
45. **Perreault M, Marette A.** Targeted disruption of inducible nitric oxide synthase protects against obesity-linked insulin resistance in muscle. *Nat Med* 7: 1138–1143, 2001.
46. **Petruschke T, Hauner H.** Tumor necrosis factor-alpha prevents the differentiation of human adipocyte precursor cells and causes delipidation of newly developed fat cells. *J Clin Endocrinol Metab* 76: 742–747, 1993.
47. **Pickup JC, Mattock MB, Chusney GD, Burt D.** NIDDM as a disease of the innate immune system: association of acute-phase reactants and interleukin-6 with metabolic syndrome X. *Diabetologia* 40: 1286–1292, 1997.
48. **Poulain-Godefroy O, Froguel P.** Preadipocyte response and impairment of differentiation in an inflammatory environment. *Biochem Biophys Res Commun* 356: 662–667, 2007.
49. **Rhen T, Cidlowski JA.** Antiinflammatory action of glucocorticoids–new mechanisms for old drugs. *N Engl J Med* 353: 1711–1723, 2005.
50. **Roberge C, Carpentier AC, Langlois MF, Baillargeon JP, Ardilouze JL, Maheux P, Gallo-Payet N.** Adrenocortical dysregulation as a major player in insulin resistance and onset of obesity. *Am J Physiol Endocrinol Metab* 293: E1465–E1478, 2007.
51. **Sakaue H, Ogawa W, Matsumoto M, Kuroda S, Takata M, Sugimoto T, Spiegelman BM, Kasuga M.** Posttranscriptional control of adipocyte differentiation through activation of phosphoinositide 3-kinase. *J Biol Chem* 273: 28945–28952, 1998.
52. **Sandeep TC, Andrew R, Homer NZ, Andrews RC, Smith K, Walker BR.** Increased in vivo regeneration of cortisol in adipose tissue in human obesity and effects of the 11beta- hydroxysteroid dehydrogenase type 1 inhibitor carbenoxolone. *Diabetes* 54: 872–879, 2005.
53. **Schaffler A, Scholmerich J, Buchler C.** Mechanisms of disease: adipocytokines and visceral adipose tissue–emerging role in intestinal and mesenteric diseases. *Nat Clin Pract Gastroenterol Hepatol* 2: 103–111, 2005.
54. **Seckl JR, Walker BR.** Minireview: 11beta-hydroxysteroid dehydrogenase type 1- a tissue-specific amplifier of glucocorticoid action. *Endocrinology* 142: 1371–1376, 2001.
55. **Smoak KA, Cidlowski JA.** Mechanisms of glucocorticoid receptor signaling during inflammation. *Mech Ageing Dev* 125: 697–706, 2004.
56. **Straub RH, Hense HW, Andus T, Scholmerich J, Riegger GA, Schunkert H.** Hormone replacement therapy and interrelation between serum interleukin-6 and body mass index in postmenopausal women: a population-based study. *J Clin Endocrinol Metab* 85: 1340–1344, 2000.
57. **Tchkonia T, Giorgadze N, Pirtskhalava T, Thomou T, DePonte M, Koo A, Forse RA, Chinnappan D, Martin-Ruiz C, von Zglinicki T, Kirkland JL.** Fat depot-specific characteristics are retained in strains derived from single human preadipocytes. *Diabetes* 55: 2571–2578, 2006.
58. **Tilg H, Moschen AR.** Adipocytokines: mediators linking adipose tissue, inflammation and immunity. *Nat Rev Immunol* 6: 772–783, 2006.
59. **Tontonoz P, Hu E, Graves RA, Budavari AI, Spiegelman BM.** mPPAR gamma 2: tissue-specific regulator of an adipocyte enhancer. *Genes Dev* 8: 1224–1234, 1994.
60. **Ulick S, Tedde R, Mantero F.** Pathogenesis of the type 2 variant of the syndrome of apparent mineralocorticoid excess. *J Clin Endocrinol Metab* 70: 200–206, 1990.
61. **Wake DJ, Rask E, Livingstone DE, Soderberg S, Olsson T, Walker BR.** Local and systemic impact of transcriptional up-regulation of 11beta-hydroxysteroid dehydrogenase type 1 in adipose tissue in human obesity. *J Clin Endocrinol Metab* 88: 3983–3988, 2003.
62. **Wamil M, Andrew R, Chapman KE, Street J, Morton NM, Seckl JR.** 7-oxysterols modulate glucocorticoid activity in adipocytes through competition for 11beta-hydroxysteroid dehydrogenase type. *Endocrinology* 149: 5909–5918, 2008.
63. **Weisberg SP, McCann D, Desai M, Rosenbaum M, Leibel RL, Ferrante AW Jr.** Obesity is associated with macrophage accumulation in adipose tissue. *J Clin Invest* 112: 1796–1808, 2003.
64. **Xing H, Northrop JP, Grove JR, Kilpatrick KE, Su JL, Ringold GM.** TNF alpha-mediated inhibition and reversal of adipocyte differentiation is accompanied by suppressed expression of PPARg without effects on Pref-1 expression. *Endocrinology* 138: 2776–2783, 1997.
65. **Xu H, Barnes GT, Yang Q, Tan G, Yang D, Chou CJ, Sole J, Nichols A, Ross JS, Tartaglia LA, Chen H.** Chronic inflammation in fat plays a crucial role in the development of obesity-related insulin resistance. *J Clin Invest* 112: 1821–1830, 2003.
66. **Yeager MP, Guyre PM, Munck AU.** Glucocorticoid regulation of the inflammatory response to injury. *Acta Anaesthesiol Scand* 48: 799–813, 2004.
67. **Zhang TY, Daynes RA.** Glucocorticoid conditioning of myeloid progenitors enhances TLR4 signaling via negative regulation of the phosphatidylinositol 3-kinase-Akt pathway. *J Immunol* 178: 2517–2526, 2007.

p300 Plays a Critical Role in Maintaining Cardiac Mitochondrial Function and Cell Survival in Postnatal Hearts

Yasuaki Nakagawa, Koichiro Kuwahara, Genzo Takemura, Masaharu Akao, Masashi Kato, Yuji Arai, Makoto Takano, Masaki Harada, Masao Murakami, Michio Nakanishi, Satoru Usami, Shinji Yasuno, Hideyuki Kinoshita, Masataka Fujiwara, Kenji Ueshima, Kazuwa Nakao

Rationale: It is known that the transcriptional coactivator p300 is crucially involved in the differentiation and growth of cardiac myocytes during development. However, the physiological function of p300 in the postnatal hearts remains to be characterized.

Objective: We have now investigated the physiological function of p300 in adult hearts.

Methods and Results: We analyzed transgenic mice exhibiting cardiac-specific overexpression of a dominant-negative p300 mutant lacking the C/H3 domain (p300ΔC/H3 transgenic [TG] mice). p300ΔC/H3 significantly inhibited p300-induced activation of GATA- and myocyte enhancer factor 2–dependent promoters in cultured ventricular myocytes, and p300ΔC/H3-TG mice showed cardiac dysfunction that was lethal by 20 weeks of age. The numbers of mitochondria in p300ΔC/H3-TG myocytes were markedly increased, but the mitochondria were diminished in size. Moreover, cardiac mitochondrial gene expression, mitochondrial membrane potential and ATP contents were all significantly disrupted in p300ΔC/H3-TG hearts, suggesting that mitochondrial dysfunction contributes to the progression of the observed cardiomyopathy. Transcription of peroxisome proliferator-activated receptor γ coactivator (PGC)-1α, a master regulator of mitochondrial gene expression, and its target genes was significantly downregulated in p300ΔC/H3-TG mice, and p300ΔC/H3 directly repressed myocyte enhancer factor 2C-dependent PGC-1α promoter activity and disrupted the transcriptional activity of PGC-1α in cultured ventricular myocytes. In addition, myocytes showing features of autophagy were observed in p300ΔC/H3-TG hearts.

Conclusions: Collectively, our findings suggest that p300 is essential for the maintenance of mitochondrial integrity and for myocyte survival in the postnatal left ventricular myocardium. (*Circ Res.* 2009;105:746-754.)

Key Words: mitochondrial function ■ autophagy ■ transcription ■ cardiac dysfunction

The transcriptional coactivator p300 interacts directly with components of the basal transcriptional apparatus and various enhancer-binding proteins, thereby modulating enhancer-mediated transcription.[1,2] Several lines of evidence suggest that p300 plays a critical role in the differentiation and growth of cardiac myocytes during development. For example, mice lacking a functional p300 gene die in utero, between embryonic days 9 and 11.5, because of disruption of cardiac muscle differentiation and trabeculation.[3] Within the myocardium, p300 serves as a coactivator of several transcription factors enriched in cardiac tissue, including GATA-4, myocyte enhancer factor (MEF)2, and serum response factor, and is required for these factors to exhibit their full transcriptional activities.[4–6] Notably, these molecules are also known to function as hypertrophy-responsive transcription factors during the pathogenesis of cardiac hypertrophy and heart failure in adults, and transgenic mice expressing p300 under the control of the cardiac-specific α-myosin heavy chain (MHC) promoter exhibit eccentric cardiac hypertrophy and increased mortality,[7] whereas cardiac-specific overexpression of p300 exacerbates adverse cardiac remodeling after myocardial infarction.[8] These findings imply that in some cases a therapeutic benefit may be obtained through inhibition of p300.[9] On the other hand, p300 appears to be essential for normal cardiac development[3,10] and important for cardiac myocyte survival under some conditions.[11]

Original received April 4, 2008; resubmission received July 28, 2009; revised resubmission received August 24, 2009; accepted August 25, 2009.

From the Department of Medicine and Clinical Science (Y.N., K.K., M.H., M.M., M.N., S.U., S.Y., H.K., M.F., K.N.), Department of Cardiovascular Medicine (M.A., M.K.), and EBM Research Center (K.U.), Kyoto University Graduate School of Medicine; Department of Cardiology and Respirology, Regeneration and Advanced Medical Sciences (G.T.), Graduate School of Medicine, Gifu University; Department of Bioscience (Y.A.), National Cardiovascular Center Research Institute, Suita; and Department of Biophysics (M.T.), Jichi Medical School, Shimotsuke, Japan.

Correspondence to Koichiro Kuwahara, Department of Medicine and Clinical Science, Kyoto University Graduate School of Medicine, 54, Shogoin-Kawara-cho, Sakyo-ku, Kyoto 606-8507, Japan. E-mail kuwa@kuhp.kyoto-u.ac.jp

Circulation Research is available at http://circres.ahajournals.org

DOI: 10.1161/CIRCRESAHA.109.206037

Consequently, inhibiting the activity of p300 could have adverse effects on the adult heart.

Peroxisome proliferator-activated receptor (PPAR)γ coactivator (PGC)-1α,[12] estrogen-related receptor (ERR)α,[13] and PPARα[14] are 3 mediators recently shown to regulate mitochondrial biogenesis and gene expression.[15] PGC-1α was cloned based on its ability to interact with PPARγ[16] and appears to be a critical regulator involved in the control of cardiac mitochondrial function in response to energy demands.[12] ERRα reportedly acts as an effector of PGC-1α and is an important regulator of genes involved in oxidative phosphorylation and mitochondrial biogenesis.[17] Furthermore, PPARα was shown to regulate expression of genes involved in mitochondrial fatty acid oxidation.[14] It is known that p300 forms complexes with PGC-1α and PPARα,[18–20] but the precise function of p300 in mitochondrial gene expression and function remains unclear.

Our aim in the present study was to examine the physiological function of p300 in the postnatal heart. To accomplish that, we developed a transgenic (TG) mouse that overexpresses a dominant-negative p300 mutant lacking the C/H3 domain (p300ΔC/H3) under the control of the cardiac-specific α-MHC promoter. Notably, these p300ΔC/H3 transgenic (p300ΔC/H3-TG) mice showed severe cardiomyopathy and died prematurely, and our findings demonstrate that p300 is essential for the maintenance of mitochondrial integrity and for the survival of cardiac myocytes in the postnatal heart.

Non-standard Abbreviations and Acronyms

ANP	atrial natriuretic peptide
BNP	brain natriuretic peptide
ERRα	estrogen-related receptor α
H&E	hematoxylin/eosin
LC3	microtubule-associated protein 1 light chain 3
LV	left ventricular
MEF2	myocyte enhancer factor 2
MHC	myosin heavy chain
PGC-1α	peroxisome proliferator-activated receptor γ coactivator-1α
PPAR	peroxisome proliferator-activated receptor
SERCA2	sarcoplasmic/endoplasmic reticulum calcium ATPase 2
SRPK3	serine/arginine-rich protein–specific kinase 3
TG	transgenic
TMRE	tetramethylrhodamine ethyl ester
WT	wild type

Methods

Plasmid Constructs

A fragment containing full-length wild-type (WT) p300 or p300ΔC/H3, in which the C/H3 domain was deleted, was inserted into the pCMVβ. Constructs containing the luciferase gene driven by the −452 bp of the proximal enhancer–promoter region of the atrial natriuretic peptide (ANP) gene (−452hANPluc) or by the −1812 bp of the enhancer-promoter region of the brain natriuretic peptide (BNP) gene (−1812hBNPluc) were described previously.[21,22] Luciferase reporter genes driven by the promoter region of the PCG1α gene, tandem GATA sites (GATA-luc), and tandem MEF2 sites (3xMEF2-luc) were kindly provided by M. D. Schneider (Baylor College of Medicine, Houston, Tex), R. S. Viger (University Laval, Ontario, Canada), and E. N. Olson (University of Texas Southwestern Medical Center, Dallas, Tex), respectively. A luciferase reporter gene driven by multiple PPAR response element sites and an expression vector encoding ERRα were kindly provided by D. P. Kelly (Washington University, St Louis, Mo).

Cell Culture, Transfection, and Luciferase Assay

Neonatal rat ventricular myocytes were prepared and transiently transfected by electroporation as described previously.[23,24]

Western Blotting Analysis

To evaluate autophagy, we used an antimicrotubule-associated protein 1 light chain 3 (LC3) antibody kindly provided by N. Mizushima (Tokyo Medical and Dental University, Japan)[25,26] and an anti–cathepsin D antibody (Santa Cruz Biotechnology).

Tetramethylrhodamine Ethyl Ester Staining of Isolated Adult Mouse Cardiomyocytes and Whole Hearts Ex Vivo

Isolated ventricular myocytes were suspended in DMEM supplemented with 10 mmol/L HEPES and plated in 6-well dishes. Tetramethylrhodamine ethyl ester (TMRE) (100 nmol/L; Molecular Probes, Eugene) was then added to the medium for 30 minutes, after which the intensity of TMRE fluorescence was evaluated using confocal microscopy.

For TMRE staining of whole hearts ex vivo, we analyzed Langendorff-perfused mouse hearts using a modification of the Langendorff method previously described for use with rat hearts.[27]

Statistical Analysis

Data are presented as means±SEM. Unpaired t tests were used for comparisons between 2 groups, and ANOVA with post hoc Fisher's tests was used for comparison among groups. Values of $P<0.05$ were considered significant.

An expanded Methods section is available in the Online Data Supplement at http://circres.ahajournals.org.

Results

p300ΔC/H3 Inhibits the Activities of Cardiac Transcription Factors and Cardiac Gene Transcription in a Dominant-Negative Fashion

A well-conserved C/H3 domain is necessary for the interaction of p300 with multiple DNA-binding factors,[4,28–30] and p300 lacking its C/H3 domain reportedly acts as a dominant-negative mutant.[2] With that in mind, we initially tested whether a p300 C/H3 deletion mutant (p300ΔC/H3) would exert a dominant-negative effect on the cardiac-enriched transcription factors MEF2 and GATA4, both of which are known to functionally interact with p300.[4,28] p300ΔC/H3 dose-dependently inhibited GATA 4- and MEF 2-induced transcriptional activation of the reporter genes (Figure 1A and 1B), and also inhibited p300-induced enhancement of GATA4- and MEF2-mediated transcription, confirming its dominant-negative effect (Figure 1C and 1D).

To examine the effect of p300ΔC/H3 on the expression of cardiac genes, we cotransfected cultured rat neonatal ventricular myocytes with p300ΔC/H3 and −452hANPLuc or −1812hBNPLuc, and found that p300ΔC/H3 dose-dependently inhibited the activities of both −452hANPLuc and−1812hBNPLuc (Figure 1E and 1F), as well as GATA4-

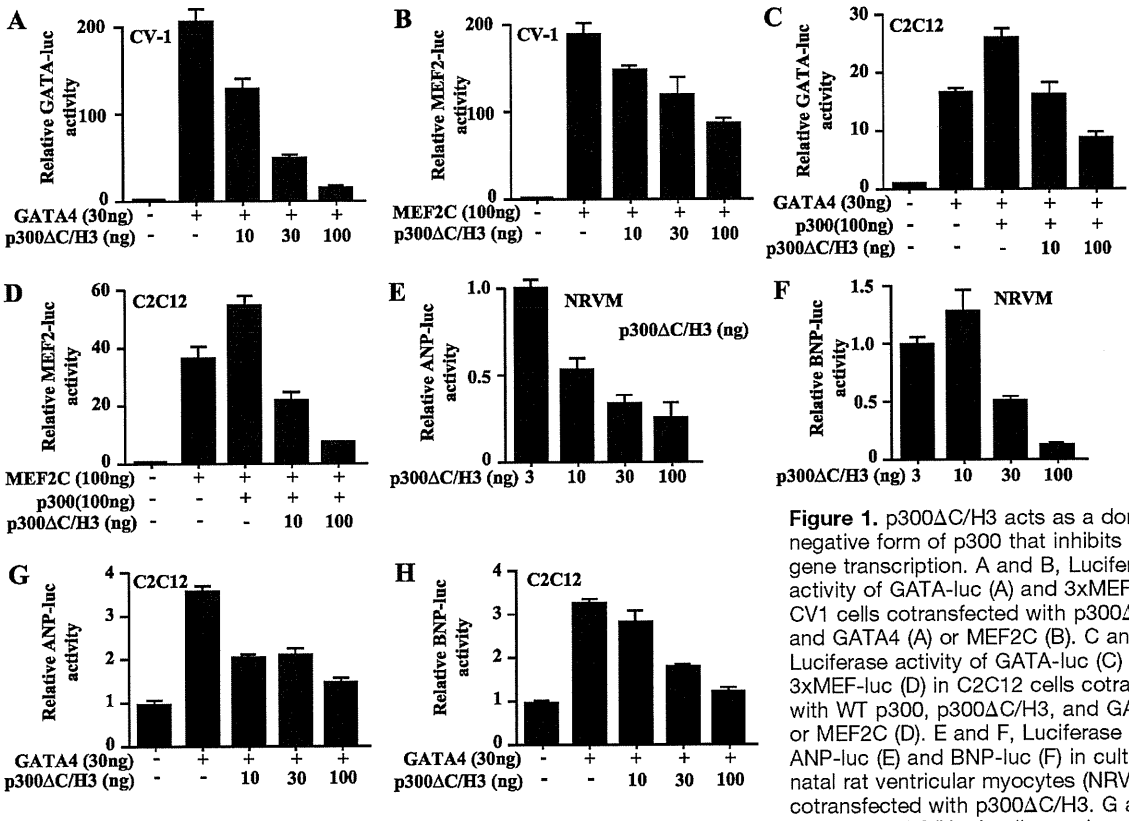

Figure 1. p300ΔC/H3 acts as a dominant negative form of p300 that inhibits cardiac gene transcription. A and B, Luciferase activity of GATA-luc (A) and 3xMEF-luc (B) in CV1 cells cotransfected with p300ΔC/H3 and GATA4 (A) or MEF2C (B). C and D, Luciferase activity of GATA-luc (C) and 3xMEF-luc (D) in C2C12 cells cotransfected with WT p300, p300ΔC/H3, and GATA4 (C) or MEF2C (D). E and F, Luciferase activity of ANP-luc (E) and BNP-luc (F) in cultured neonatal rat ventricular myocytes (NRVM) cotransfected with p300ΔC/H3. G and H, Luciferase activity of ANP-luc (G) and BNP-luc (H) in C2C12 cells cotransfected with GATA4 and p300ΔC/H3. In all experiments, luciferase activities in cells transfected with the reporter construct alone were assigned a value of 1.0. Bars represent means±SEM.

induced activation of −452hANPLuc and −1812hBNPLuc in C2C12 cells (Figure 1G and 1H).

Cardiac Overexpression of p300ΔC/H3 Causes Heart Failure and Premature Death

Having confirmed the dominant-negative effect of p300ΔC/H3, we sought to evaluate the physiological function of p300 in adult heart using p300ΔC/H3-TG mice, in which p300ΔC/H3 was expressed under the control of the cardiac-specific αMHC promoter (Figure 2A). We obtained and investigated 2 independently derived p300ΔC/H3-TG founders (TG1 and TG2). The data obtained from TG1 were essentially the same as those obtained from TG2 shown in Online Figure I (A through H) and are presented below. Expression of the protein encoded by the transgene was confirmed by Western blotting with an anti-hemagglutinin tag antibody (Figure 2B). Moreover, Western blotting with antibodies recognizing both WT mouse p300 and mutant human p300ΔC/H3 showed that the level of p300ΔC/H3 expression was 1.9-fold higher than that of endogenous p300 (Figure 2C).

p300ΔC/H3-TG mice appeared normal at birth, but by 12 weeks after birth, their survival rate was significantly lower than that of WT mice (survival rate at 12 weeks of age: WT [n=40], 100%; TG [n=28], 71%; Figure 2D), and almost all had died by 20 weeks of age (survival rate at 20 weeks of age: WT [n=40], 100%; TG [n=28], 3.5%; Figure 2D). The survival rate among p300ΔC/H3-TG mice was also much lower than that among TG mice overexpressing exogenous WT p300 in their hearts, which showed 76% survival at 42 weeks of age.[7] At 12 weeks of age, the hearts of p300ΔC/H3-TG mice were much larger than those of WT mice (Figure 2E, 2F and 2G). Likewise, the lung weight/body weight ratios were significantly higher in p300ΔC/H3-TG mice (Figure 2H). Echocardiographic analysis revealed the ejection fraction to be significantly reduced and the left ventricular (LV) end-systolic diameter to be significantly increased in p300ΔC/H3-TG mice (Table). In another transgenic mouse, TG2, which expressed the transgene at a lower level than TG1, we found similar but milder LV dysfunction and dilatation (Online Figure I, A through F). Hemodynamic analysis of 12-week-old p300ΔC/H3-TG mice also indicated LV dysfunction, as reflected by markedly elevated LV end-diastolic pressure and significant depression of both the maximal and minimal rates of LV pressure development (dP/dt-max and dP/dt-min, respectively) (Table).

When we then used real-time PCR to examine the expression of cardiac stress markers in p300ΔC/H3-TG mice, we found that expression of both ANP and BNP was markedly upregulated, and expression of sarcoplasmic/endoplasmic reticular calcium ATPase (SERCA)2 was significantly downregulated in p300ΔC/H3-TG hearts (Figure 2I through 2K; Online Figure I, G).[31,32] Although p300ΔC/H3 inhibited ANP and BNP gene transcription in cultured cardiac myocytes, this suggests that endogenous p300 is

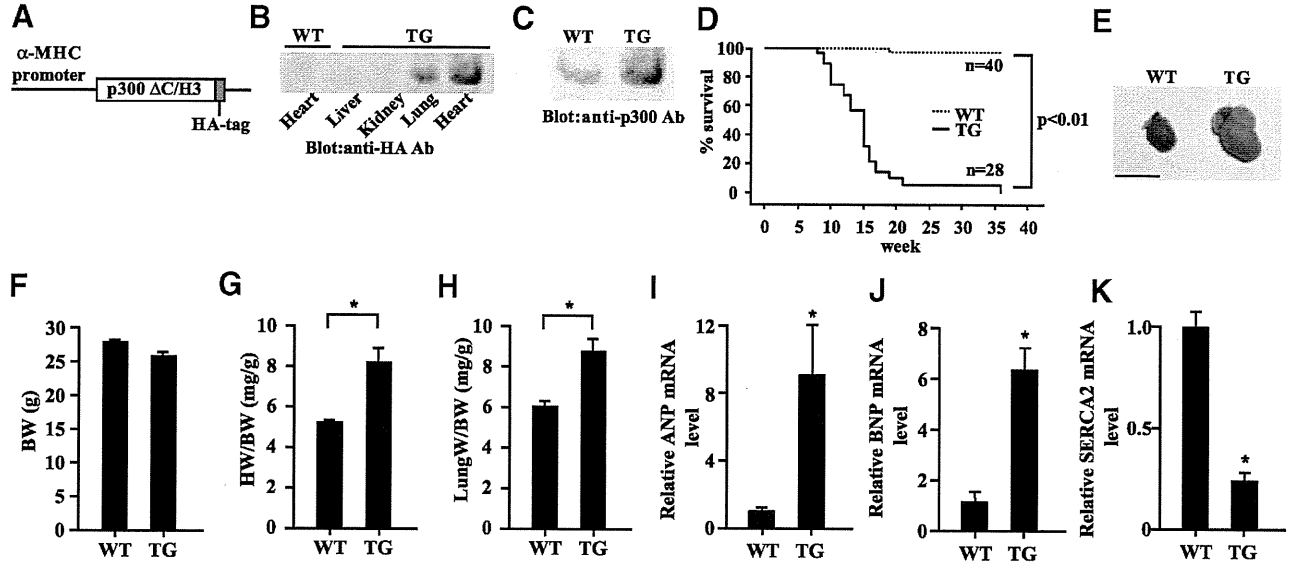

Figure 2. Premature death and cardiomyopathy in p300ΔC/H3-TG mice. A, Schematic representation of the construct for the αMHC-p300ΔC/H3 transgene. B, Western blot analysis of p300ΔC/H3 in the indicated tissue was performed using anti-hemagglutinin (HA) antibody. C, Western blot analysis of WT mouse p300 and mutant human p300ΔC/H3 in the heart was performed using an antip300 antibody able to detect both WT mouse p300 and mutant human p300ΔC/H3. D, Kaplan–Meier survival analysis of p300ΔC/H3-TG and WT mice showing a significant difference in survival rates. E, Gross appearance of hearts from 12-week-old p300ΔC/H3-TG and WT mice. Scale bars=10 mm. F through H, Body weights (BW) (F), heart weight/body weight (HW/BW) ratios (G), and lung weight/body weight ratios (LuW/BW) (H) in 12-week-old p300ΔC/H3-TG and WT mice. *$P<0.05$. I through K, Relative levels of ANP (I), BNP (J), and SERCA2 (K) mRNA quantified by real-time RT-PCR in ventricles of WT and p300ΔC/H3-TG hearts. *$P<0.05$ vs WT. Relative mRNA levels in WT were assigned a value of 1.0. Bars represent means±SEM.

not required for pathological induction of these fetal cardiac genes in adult hearts.

Histological examination of cross-sections confirmed enlargement of the atrial and ventricular chambers in 12-week-old p300ΔC/H3-TG hearts (Figure 3A, 3B, 3C, and 3D). At higher magnification, hematoxylin/eosin (H&E)-stained ventricular myocytes from p300ΔC/H3-TG hearts were highly variable in size (Figure 3E and 3F). In addition, Sirius red staining revealed the presence of significant interstitial fibrosis in p300ΔC/H3-TG ventricles (Figure 3G and 3H), whereas electron microscopic examination revealed vacuolization of the ventricular myocytes and myofibrillar degeneration, features typical of human cardiomyopathy (Figure 3I). We also performed oil-O-red staining to compare the lipid droplets in the ventricular myocardia of WT and p300ΔC/H3-TG mice and found there to be no difference between the 2 genotypes (data not shown).

Table. Echocardiographic and Hemodynamic Analysis in 12-Week-Old WT and p300ΔC/H3-TG Mice

Analysis	Wild Type	Transgenic	*P*
Echographic data			
N	8	11	
LVDd (mm)	4.24±0.63	5.26±0.11	<0.0001
LVDs (mm)	3.05±0.07	4.61±0.14	<0.0001
IVST (mm)	0.63±0.04	0.56±0.04	0.202
PWT (mm)	0.59±0.03	0.56±0.41	0.555
FS (%)	29.88±0.93	12.82±1.20	<0.0001
EF (%)	65.50±1.48	33.09±2.59	<0.0001
Hemodynamic data			
N	3	3	
LVSP (mm Hg)	100.07±0.87	86.67±8.75	0.202
LVEDP (mm Hg)	5.87±0.353	2.93±3.733	0.133
dP/dt (mm Hg/sec)	4913.33±96.84	3768.00±322.86	0.0274
−dP/dt (mm Hg/sec)	−5146.67±327.48	−2853.33±233.33	0.0047
HR (bpm)	581.67±18.33	481.67±42.33	0.0242

Values are means±SEM. dP/dt indicates first derivative of pressure; EF, ejection fraction; FS, fractional shortening; HR, heart rate; IVST, interventricular septal thickness; LVEDP, left ventricular end diastolic pressure; LVDd, left ventricular end diastolic dimension; LVDs, left ventricular end systolic diameter; LVSP, left ventricular systolic pressure; PWT, posterior wall thickness.

p300ΔC/H3 Directly Inhibits the Expression and Function of PGC-1α

Electron microscopic examination also revealed that the numbers of mitochondria were dramatically increased in p300ΔC/H3-TG myocytes, but that they were much smaller in size than those in WT myocytes (Figure 3I). This prompted us to assess the expression and function of mitochondrial genes in p300ΔC/H3-TG mice. Using quantitative real-time RT-PCR, we evaluated the transcription of genes related to mitochondrial fatty acid oxidation and mitochondrial replication. Expression of nuclear respiratory factor (NRF)1 and mitochondrial transcription factor A mRNAs was significantly downregulated in p300ΔC/H3-TG hearts, as compared to WT hearts (Figure 4A). Expression of genes involved in fatty acid oxidation, including carnitine palmitoyltransferase-I and -II and medium- and long-chain acyl-coenzyme A

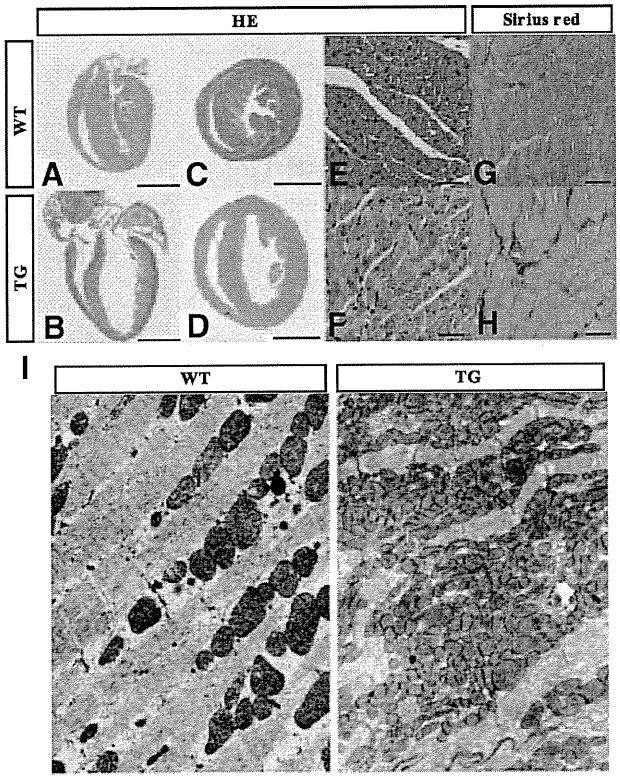

Figure 3. Pathological changes in p300ΔC/H3-TG hearts. A through H, Histological analysis of hearts from 12-week-old p300ΔC/H3-TG and WT mice. A through D, Hearts from WT (A and C) and p300ΔC/H3-TG (B and D) mice were sectioned longitudinally (A and B) or coronally (C and D) and stained with H&E. Scale bars=2.5 mm. E through H, Higher magnification of histological sections of WT (E and G) and p300ΔC/H3-TG (F and H) hearts stained with H&E (E and F) or Sirius red (G and H). Scale bars=50 μm. I, Transmission electron micrographs of cardiac myocytes from 12-week-old WT (left) and p300ΔC/H3-TG (right) hearts.

dehydrogenase, was also diminished in P300ΔC/H3-TG hearts (Figure 4A; Online Figure I, H). Given these reductions in mitochondrial gene expression in p300ΔC/H3-TG hearts, we also evaluated the expression of genes encoding PGC-1α, ERRα, and PPARα, 3 mediators thought to be involved in regulating mitochondrial gene expression. As shown in Figure 4B and Online Figure I (H), expression of all 3 was significantly downregulated in p300ΔC/H3-TG mice.

It was recently reported that PGC-1α induces the expression of ERRα and then interacts with the expressed protein, enabling it to activate transcription.[17] In addition, ERRα reportedly activates PPARα gene expression by directly binding to the PPARα promoter.[13] Therefore, to determine whether p300ΔC/H3 directly inhibits transcription of PGC-1α, the upstream activator of ERRα and PPARα, we carried out reporter assays using a PGC-1α promoter-luciferase reporter gene. In neonatal rat ventricular myocytes, p300ΔC/H3 significantly and dose-dependently inhibited the activity of the PGC-1α promoter (Figure 4C).

Because MEF2, a muscle-enriched transcriptional activator that interacts with p300, was previously shown to regulate PGC-1α promoter activity,[33,34] we next tested the effect of p300ΔC/H3 on MEF2C-inducible PGC-1α promoter activity in CV1 cells. We found that MEF2C-induced PGC-1α promoter activity was significantly inhibited by p300ΔC/H3 (Figure 4D), suggesting that p300ΔC/H3 directly inhibits PGC-1α gene expression in p300ΔC/H3-TG hearts. The mRNA expression of serine/arginine-rich protein–specific kinase (SRPK)3, another MEF2 target gene, was also significantly downregulated in p300ΔC/H3-TG hearts (Figure 4E). In addition, because p300 reportedly acts as a coactivator of PGC-1α and ERRα, we also tested whether p300ΔC/H3 directly inhibits PGC-1α-mediated activation of ERRα, which would in turn inhibit PPARα gene expression. That p300ΔC/H3 significantly inhibited PGC-1α- and ERRα-induced activation of the PPARα promoter (Figure 4F) means that p300ΔC/H3 exerts inhibitory effects on both the expression and function of PGC-1α, thereby suppressing expression of multiple mitochondrial genes in p300ΔC/H3-TG mice.

Abnormal Mitochondrial Function in p300ΔC/H3-TG Hearts

To evaluate the function of mitochondria in p300ΔC/H3-TG hearts, we initially stained isolated ventricular myocytes with TMRE, a fluorescent dye whose accumulation in active mitochondria is dependent on the mitochondrial membrane potential. Examination of individual mitochondria revealed that TMRE fluorescence reflecting the mitochondrial membrane potential was disorganized and sparse, whereas mean TMRE signals from individual mitochondria were significantly weaker in ventricular myocytes isolated from p300ΔC/H3-TG mice than in those from WT mice (Figure 5A and 5B). We also used 2-photon laser microscopy to examine the mitochondrial membrane potential ex vivo in Langendorff-perfused p300ΔC/H3-TG hearts.[27] Again the fluorescent signals from the mitochondria in p300ΔC/H3-TG myocytes were significantly weaker than those from WT myocytes (Figure 5C and 5D), which confirmed the disruption of mitochondrial function in p300ΔC/H3-TG hearts. In addition, we subjected p300ΔC/H3-TG and WT hearts perfused with TMRE to global ischemia by clamping off the perfusion line and then monitored TMRE fluorescence in the ischemic hearts (Figure 5E). We observed a time-dependent loss of TMRE fluorescence, indicating depolarization of the mitochondrial membrane, in all of the ischemic hearts (Figure 5F). Notably, however, both the time course of the change in TMRE fluorescence (Figure 5F) and the average TMRE signals from individual cells (Figure 5G and 5H) in WT and p300ΔC/H3-TG hearts subjected to ischemia clearly showed that the depolarization was significantly greater in p300ΔC/H3-TG hearts than in WT hearts (Figure 5F, 5G and 5H). Moreover, the ATP content of p300ΔC/H3-TG hearts was significantly lower than in WT hearts (Figure 5I).

Increased Autophagic Myocardial Cell Death in p300ΔC/H3-TG

Mitochondrial dysfunction can lead to cell death through induction of apoptosis by release of cytochrome *c* and

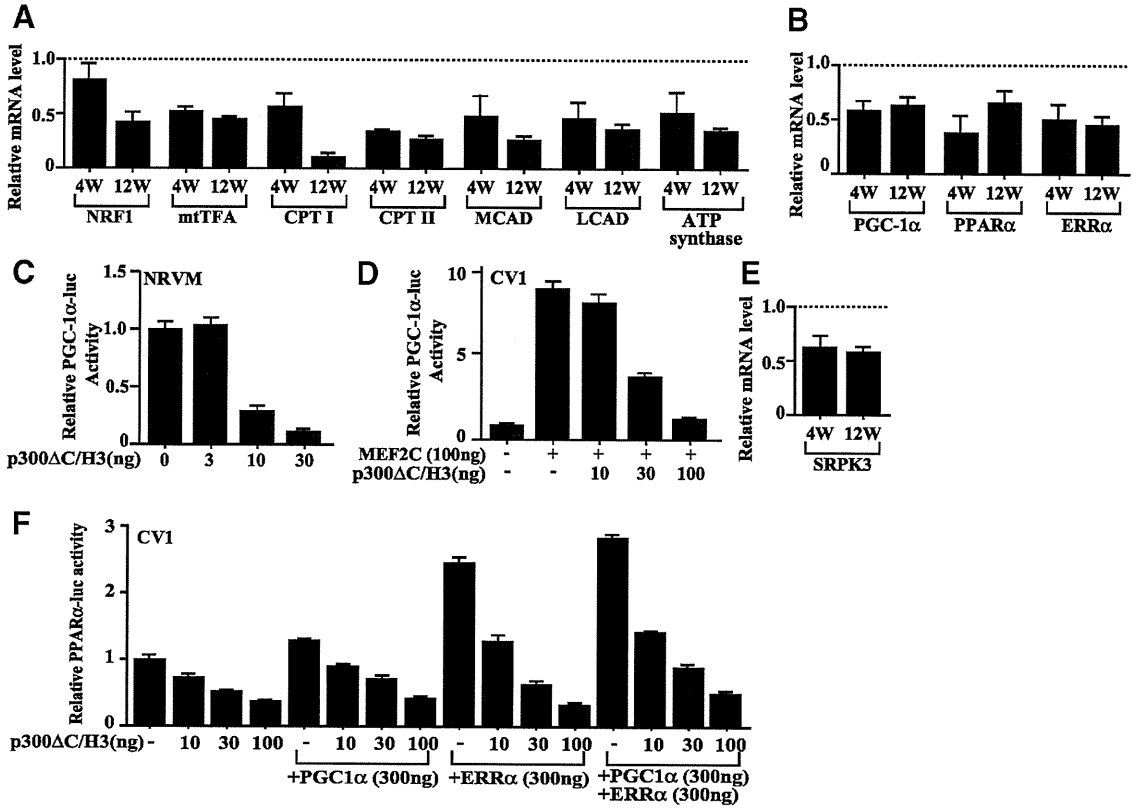

Figure 4. Reduced expression of mitochondrial genes in p300ΔC/H3-TG ventricles. A and B, Levels of mRNA expression of mitochondrial genes in p300ΔC/H3-TG normalized to the level in WT hearts were examined using real-time quantitative RT-PCR. The graphs show the relative levels of the indicated mRNAs normalized to the level of GAPDH mRNA in p300ΔC/H3-TG hearts and then further normalized to the levels in age-matched WT controls. $P<0.05$ between WT and p300ΔC/H3-TG hearts in all genes at both 4 and 12 weeks of age. CPT indicates carnitine palmitoyltransferase; LCAD, long-chain acyl-coenzyme A dehydrogenase; MCAD, medium-chain acyl-coenzyme A dehydrogenase. C and D, Luciferase activity of PCG-1α-luc in neonatal ventricular myocytes (NRVM, C) or CV1 cells (D) cotransfected with p300ΔC/H3 (C) or p300ΔC/H3+MEF2C (D). E, Levels of SRPK3 mRNA in p300ΔC/H3-TG hearts relative to those in WT hearts were examined using real-time quantitative RT-PCR. $P<0.05$ between WT and p300ΔC/H3-TG hearts. F, Luciferase activity of PPARα-luc in CV1 cells, cotransfected with p300ΔC/H3, PGC-1α and ERRα. In all of these experiments, luciferase activities in cells transfected with the reporter construct alone were assigned a value of 1.0. In all graphs, bars represent means±SEM.

subsequent activation of the caspase cascade, or through autophagic cell death mediated by cross-talk between the mitochondria and Golgi apparatus.[35] We then carried out Evans blue dye assays to compare the incidences of myocardial cell death in p300ΔC/H3-TG and WT hearts.[36] As shown in Figure 6A and 6B, intraperitoneally injected Evans blue labeled numerous cells in p300ΔC/H3-TG hearts, indicating the presence of ongoing cell death, but not in WT hearts. Electron microscopic examination of several degenerative myocytes in p300ΔC/H3-TG hearts revealed the presence of cytosolic vacuoles containing lipid droplets, myelin fibers, and degenerated mitochondria, typical features of autophagosomes (Figure 6C). Finally, Western blot analysis showed increased expression of LC3-II and cathepsin D, 2 markers of autophagic cell death, in p300ΔC/H3-TG hearts (Figure 6D). By contrast, agarose gel electrophoresis of genomic DNA provided no evidence of the DNA laddering characteristic of apoptosis (Figure 6E). In addition, there was no increase in the cleavage of caspase 3, a critical event in the activation of mitochondrial apoptotic pathways (Figure 6F).

Discussion

To evaluate the physiological function of p300 in postnatal hearts, we analyzed mice overexpressing a dominant negative p300 mutant (p300ΔC/H3) under the control of the α-MHC promoter. We found that LV function was disrupted in p300ΔC/H3-TG mice and that almost all died of heart failure by 20 weeks of age. p300ΔC/H3-TG hearts showed several mitochondrial abnormalities affecting both their structure and function. Expression of PGC-1α, a master regulator of mitochondrial gene expression,[15] and its target genes were markedly diminished in p300ΔC/H3-TG hearts. p300ΔC/H3 directly inhibited both the expression of PGC-1α and its transcriptional activity and also inhibited the transcriptional activity of ERRα, another regulator of mitochondrial gene expression. Consistent with these findings, mitochondrial membrane potential was severely depolarized in p300ΔC/H3-TG mice. Thus p300 appears to play an essential role in maintaining mitochondrial integrity in postnatal hearts, and its inhibition in adult hearts can lead to mitochondrial and LV dysfunction and death.